Identification of various types of α2-HS glycoprotein in sera of patients with pancreatic cancer: Possible implication in resistance to protease treatment

KANA KUWAMOTO[1], YURI TAKEDA[1], AKIKO SHIRAI[2], TSUTOMU NAKAGAWA[1], SHUNSAKU TAKEISHI[3], SHINJI IHARA[5], YASUHIDE MIYAMOTO[4], SHINICHIRO SHINZAKI[1], JEONG HEON KO[6] and EIJI MIYOSHI[1]

[1]Department of Molecular Biochemistry and Clinical Investigation, Osaka University Graduate School of Medicine; [2]DS Pharma Biomedical Co. Ltd. Research and Development Department; [3]GPBio Science Corp; [4]Osaka Medical Center for Cancer and Cardiovascular Diseases, Japan; [5]Department of Biology, Duke University, Durham, NC 27708, USA; [6]Daejeon-KRIBB-FHCRC Research Cooperation Center, Daejeon 305-806, Korea

Received March 17, 2010; Accepted May 11, 2010

DOI: 10.3892/mmr_00000311

Abstract. α2-Heremans-Schmid glycoprotein (human fetuin) is one of numerous serum proteins produced in the liver. Recently, the biological functions of fetuin, such as calcification and insulin resistance, have been clarified. However, these effects appear to be indirect, occurring through binding to other molecules. When equal amounts of fetuin in sera were treated with chymotrypsin, resistance to the protease treatment was observed in patients with pancreatic cancer, but not in normal volunteers. To investigate the molecular mechanism behind this resistance, gel-filtration chromatography was performed. The results revealed that high molecular types of fetuin showed a resistance to protease treatment. When fetuin was purified from sera of patients with pancreatic cancer and normal volunteers, certain types of proteins, including haptoglobin (which binds to fetuin derived from pancreatic cancer patients), were identified using mass spectrometry. Furthermore, the oligosaccharide structures of fetuin analyzed with lectin microarray differed between pancreatic cancer patients and normal volunteers. This macro/micro heterogeneity of fetuin might contribute to pancreatic cancer resistance to chymotrypsin treatment.

Introduction

α2-Heremans-Schmid glycoprotein (AHSG, human fetuin) is one of the plasma proteins that occur in high concentrations during fetal life and gradually decrease towards adulthood. However, fetuin remains abundant in adult serum, and is mostly produced in the liver (1,2). Previous studies have demonstrated that fetuin isolated from Cohn's fraction VI of human plasma is a two-chain molecule consisting of an A-chain of 282 amino acid residues and a B-chain of 27 residues (3,4). It is thought that the circulating form of fetuin in serum is a two-chain protein with a heavy chain of 321 residues, which indicates the A chain with the connecting peptide, and a light chain of 27 residues, which indicates the B chain (5). Jahnen Dechent W *et al* reported that chymotrypsin cleaved the critical Leu-Leu bond flanking the NH_2-terminal portion of the connecting peptide region, and that this proteolysis was accelerated in sera of patients with sepsis (6).

Fetuin is a glycoprotein with both N- and O-linked carbohydrate side chains whose structures vary in several biological aspects (7,8). Fetuin occurs in large amounts in blood and cerebrospinal fluid, accumulates to high concentrations in calcified bone, and is involved in the regulation of mineral concentration (9). Since fetuin belongs to one of the negative acute-phase proteins, levels of fetuin in serum are decreased in individuals with infections, malignancies, malnutrition and liver and renal diseases at the end stage (10-13). Its high affinity for bone mineral and ability to prevent the precipitation of basic calcium phosphates from supersaturated solutions suggest that fetuin is a potent systemic inhibitor of soft tissue calcification (14-17). As there is a similarity in anion acid structures between fetuin and TGF-β receptor, fetuin acts as an antagonist of TGF-β. By contrast, it was reported that fetuin acted as a natural inhibitor of the insulin receptor tyrosine kinase in liver and skeletal muscle (18-22), and as an inhibitor for TNF-α during inflammation (23). Recent studies demonstrated that human plasma fetuin-A levels were correlated with fatty liver, impaired glucose tolerance and insulin resistance (24,25). In order to study a variety of biological functions of fetuin in detail, fetuin-deficient mice were developed. Unexpectedly, these mice showed normal growth. When fed a high-fat diet, they were resistant to weight gain, demonstrated significantly decreased body fat and remained insulin sensitive (26). However, several studies have examined the role of fetuin as a calcification inhibitor, since

Correspondence to: Dr Eiji Miyoshi, Department of Molecular Biochemistry and Clinical Investigation, Osaka University Graduate School of Medicine, 1-7, Yamada-oka, Suita 565-0871, Japan
Email: emiyoshi@sahs.med.osaka-u.ac.jp

Abbreviations: α2-Heremans-Schmid glycoprotein, human fetuin

Key words: α2-HS glycoprotein, heterogeneity, lectin array, pancreatic cancer, proteolysis

the mice developed microcalcifications in soft tissue. Fetuin is highly effective in the formation and stabilization of protein-mineral colloids, referred to as calciprotein particles (CPPs). CPPs may act as mineral chaperones mediating the stabilization, safe transport and clearance of calcium and phosphate as colloidal complexes in the body, thus preventing ectopic calcification (24,27). All these reports on fetuin suggest that fetuin may react biologically with other molecules. Therefore, it would be useful to know the heterogenic conditions of fetuin in serum, such as complex formation and binding with other proteins. In the present study, we found that the limited proteolysis of serum fetuin differed between patients with pancreatic cancer and normal volunteers. The mechanisms for the difference were investigated in terms of differences in the heterogeneity of fetuin in serum, complex formation with other molecules, and oligosaccharide structures.

Materials and methods

Western blot analysis of fetuin. A rabbit polyclonal antibody for fetuin was established as follows: briefly, a rabbit was immunized with commercial fetuin every 2 weeks. After 3 months, the total serum of the rabbit was collected. Availability of this antibody for Western blot analysis was verified using sera or conditioned medium from a hepatoma cell line. To purify the fetuin-specific antibody, the rabbit serum was applied to an affinity column that was coupled with 3 μg of fetuin after the depletion of immunoglobulin G (IgG) (Cell Signaling Technology) using the Protein G column (GE Healthcare, Amersham, UK). An 180 ng aliquot of fetuin was electrophoresed on a 10% SDS polyacrylamide gel and transferred onto a nitrocellulose membrane (Whatman, Germany). The membranes were incubated with 5% skim milk in phosphate buffered saline (PBS) for 1 h and then incubated with 1/5,000 diluted anti-human fetuin antibody, which was established by immunizing rabbits with purified human fetuin (Sigma, St. Louis, MO, USA) overnight. After washing three times with Tris-buffered saline containing 0.05% Tween 20 (TBST) (pH 7.4) for 10 min each, the membranes were incubated with peroxidase conjugated anti rabbit IgG for 40 min. After washing the membranes three times with TBS-T for 10 min each, development was performed using an Immobilon™ Western Chemiluminescent HRP Substrate (Millipore Corp., Billerica, MA, USA) according to the standard protocol.

Column chromatography. Serum (0.8 ml) was diluted with 0.1 M Tris-HCl pH 7.4 containing 7-aminoheptanoic acid at 2.4 times and was applied to a Superdex 200 pg (1.6x60 cm) column at 4˚C using FPLC systems (GE Healthcare). The elution was performed with 0.1 M Tris-HCl pH 7.4 at 0.5 ml/min conditions, and 1.0 ml of the elution was collected in each tube. The protein concentration was detected under UV light at 280 nm. The aliquot of 66-75 fractions (Superdex 200 pg chromatography) was applied to a MonoQ column (HR 5/5: equilibrated 0.1 M Tris-HCl pH 7.4) at 25˚C, then the column was washed with the buffer for 5 min at a flow rate of 1.0 ml/min and eluted for 40 min with a linear gradient of A buffer (0.1 M Tris-HCl pH 7.4) and B buffer (0.1 M Tris-HCl pH 7.4 with 1 M NaCl). The elution (1 ml) was collected in each tube and the protein concentration was detected as above.

Enzyme linked immunosorbent assay of fetuin. Fetuin levels were determined by a competitive enzyme linked immunosorbent assay (ELISA) system, which was established using polyclonal anti-human fetuin antibodies as described above. Briefly, anti human fetuin polyclonal antibody was coated as a solid phase (96-well plate). Diluted serum (1/200) and peroxidase-labeled fetuin were applied to each well and then incubated for 30 min at room temperature. After washing three times in washing buffer (0.03% Triton X-405, 0.05% Tween 80, 0.9% NaCl, 0.005 M sodium phosphate, pH 7), TMB (DAKO, Tokyo, Japan) was added to each well. After incubation for 30 min, the reaction was stopped by the addition of 5% H_2SO_4. Fetuin captured with coated antibodies in each well was recognized by the specific fetuin antibody on a solid phase, followed by the detection of the reaction signal using TMB peroxidase substrate. The signal was measured in a spectrophotometric microplate reader (Bio-Rad, Tokyo, Japan).

Limited proteolysis of fetuin by chymotrypsin and tyrpsin. Proteolysis of fetuin was carried out in PBS pH 7.2, and sera adjusted to fetuin (180 ng concentration) were incubated with various concentrations of bovine pancreatic chymotrypsin (Calbiochem) for 30 min at 37˚C. After 30 min of incubation at 37˚C, the reaction was stopped by the addition of 5 μl SDS sample buffer and boiled for 5 min at 100˚C. The samples were electrophoresed on a 10% SDS polyacrylamide gel, and then Western blot analysis was performed.

Purification of fetuin from sera of patients with pancreatic cancer and normal volunteers. To purify fetuin, 100 μl of sera was applied to an anti-fetuin affinity column coupled with 0.5 mg of anti-human fetuin antibody according to the standard protocols of HiTrap NHS-activated HP (Amersham Bioscience). This antibody was established as previously described. Fetuin bound to the antibody column was eluted with 5 ml of elution buffer (100 mM glycine, 0.5 M NaCl pH 3.0) and then neutralized with Tris.

Mass spectrometry analysis of fetuin-binding proteins. Purified fetuin fractions in the affinity column were evaporated until dry, and 200 μl of a reducing solution containing 250 mM Tris-HCl pH 8.5, 6 M guanidine hydrochloride, 2 mM EDTA and 4 mg dithiothreitol were added to the residue. The mixture was incubated at 50˚C for 1 h to reduce Cys residues. Iodoacetamide (10 mg) was added to the mixture and the reaction was allowed to proceed for 30 min at room temperature in the dark. Water (300 μl) was added to the reaction solution and the mixture was passed through a Nap-5 column (GE Healthcare) equilibrated with water to remove salts from the reducing solution and excess iodoacetamide. The elute containing S-carbamidomethylated fetuin (1 ml, in water) was evaporated until dry. An enzyme mixture of lysylendopeptidase (40 ng) and trypsin (40 ng) in 50 mM ammonium bicarbonate (100 μl) was added to the dried residue and incubated for 16 h at 37˚C. After boiling, the solution was evaporated until dry. The residue was dissolved in 20 μl of water. A 10-μl aliquot of the tryptic peptides mixture was separated by RPLC (a Cadenza CD-C18 column, 150x2.0 mm i.d.; Imtakt, Kyoto, Japan) under the following gradient conditions: mobile phases of i) 0.1% formic acid and ii) 0.1% formic acid/80% acetonitrile. The gradient elution was performed from

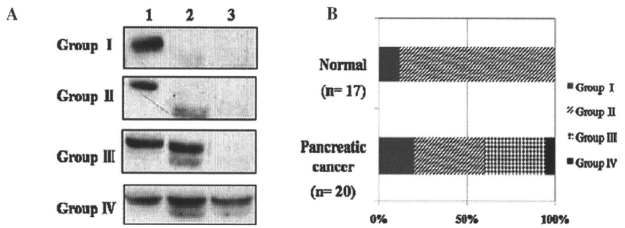

Figure 1. Proteolysis pattern of fetuin by treatment with chymotrypsin. (A) Proteolysis of fetuin was categorized into four groups (Groups I-IV). Sera adjusted by fetuin levels (180 ng) were incubated with various concentrations of bovine pancreatic chymotrypsin for 30 min at 37˚C. The chymotrypsin concentration in each lane was as follows: lane 1, 0 μg/μl; lane 2, 0.2 μg/μl; lane 3, 0.5 μg/μl. The samples were electrophoresed on a 10% SDS polyacrylamide gel, and then Western blot analysis was performed. (B) The proteolysis activity of fetuin differed between the sera of normal volunteers and pancreatic cancer patients. While normal volunteers belonged only to Groups I and II, 50% of patients with pancreatic cancer belonged to Groups III and IV, suggesting that certain cases of fetuin derived from sera of patients with pancreatic cancer were resistant to chymotrypsin treatment.

5-50% (i) over 30 min, and then from 50-100% (ii) over 10 min with a flow rate of 0.2 ml/min. The eluates were monitored at 280 nm, and continuously introduced into an electrospray ionization (ESI) source (Esquire HCT, Bruker Daltonics Inc,). The identification of the protein was performed against the NCBInr database with the MASCOT (Matrix Science Ltd.) database-searching algorithm.

Lectin microarray analysis. Lectin microarray analysis was performed as described previously (28). Briefly, ~10 ng of fetuin purified from sera of patients with pancreatic cancer and normal volunteers and conditioned medium from the human hepatoma cell line Hep3B were applied to the lectin microarray. This array is capable of comparative binding to 43 types of lectins (28). Levels of lectin binding were described as the relative intensity adjusted to the total fluorescence.

Results

Proteolysis pattern of fetuin after treatment with chymotrypsin. To investigate the limited proteolysis of fetuin in sera of patients with pancreatic cancer and normal volunteers, the serum samples were incubated with various concentrations of chymotrypsin (Fig. 1A). Certain samples were rapidly cleaved by chymotrypsin (Groups I and II). The proteolysis pattern of fetuin is categorized into four groups. While the majority of normal volunteers belonged to Groups I and II, 50% of patients with pancreatic cancer belonged to Groups III and IV, suggesting that certain patients with pancreatic cancer were resistant to chymotrypsin treatment (Fig. 1B).

Column chromatography analysis of fetuin in sera. Fetuin bands in the Western blot analysis were detected at 53 and 58 kDa, which are known as major fractions of fetuin A with and without the connecting peptide, respectively. To evaluate the dynamics of fetuin in sera, gel filtration column chromatography analysis of fetuin was performed using the serum from a patient with pancreatic cancer. Sera (0.8 ml) were applied to a Superdex (200 pg) column at 25˚C using FPLC systems. When using the sera of another pancreatic cancer patient or of normal volunteers, the fractionation pattern of fetuin was almost the same. The elution (1 ml) was collected in the tubes, and the concentration of fetuin in the fractions was determined by a competitive ELISA (Fig. 2A). The fractions of No. 65-76 peak were identified with a major band of fetuin. In contrast, except for this peak, quite low levels of fetuin were detected in a high molecular weight fraction, near No. 47-56. Western blot analysis using anti-fetuin antibody revealed that the expression levels of fetuin in each fraction of No. 54-75 were compatible with the fetuin concentration determined by a competitive ELISA (Fig. 2B).

Molecular mass of fetuin in high molecular fractions differed from that in low molecular fractions. As described previously, extremely low levels of fetuin were detected in a high molecular weight fraction. To investigate the difference between fetuin with a high molecular weight fraction and a major fraction of low molecular weight, Western blot analysis was performed under reducing conditions (Fig. 3). Notably, the molecular mass of fetuin in these two fractions was different under reducing conditions. To examine whether or not the difference in this molecular weight is dependent on glycosylation, each fraction was treated with N-endglycosidase F (PNGase). While the bands of fetuin were suppressed with PNGase treatment, there were no changes in the molecular mass of fetuin between high and low molecular fractions, suggesting that the molecular difference between the two types of fetuin was not dependent on glycosylation (data not shown).

Proteolytic pattern of the eluted fraction after treatment with chymotrypsin and trypsin. To investigate the limited proteolysis of fetuin in the high molecular weight fraction, both fractions were treated with various concentrations of chymotrypsin or trypsin. Fetuin in the low molecular fraction was cleaved by both chymotrypsin and trypsin. By contrast, the high molecular mass fetuin was resistant to chymotrypsin and trypsin treatment (Fig. 4).

Identification of fetuin-associated proteins. To examine whether or not fetuin specifically binds to other molecules in sera of patients with pancreatic cancer, we purified fetuin from sera of normal volunteers and patients with pancreatic cancer using an anti-fetuin antibody affinity column. Eluted proteins were electrophoresed on a 10% SDS polyacrylamide

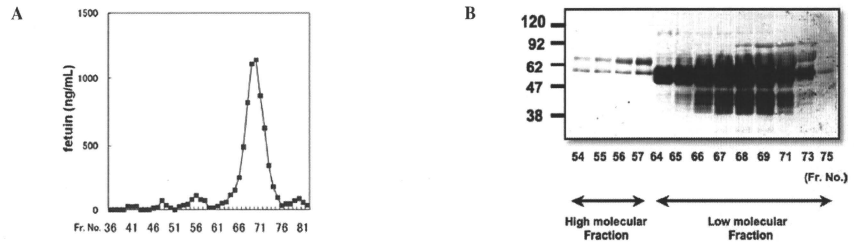

Figure 2. Column chromatography analysis of fetuin in sera. (A) Column chromatography analysis of fetuin in serum of a patient with pancreatic cancer. Sera (0.8 ml) was applied to a Superdex (200 pg) column at 25°C using FPLC systems. The elution (1 ml) was collected in the tubes. The fetuin concentration in the fractions were determined by ELISA. (B) Fraction samples (10 μl) of Nos. 54-75 were electrophoresed on a 10% polyacrylamide gel under reducing conditions.

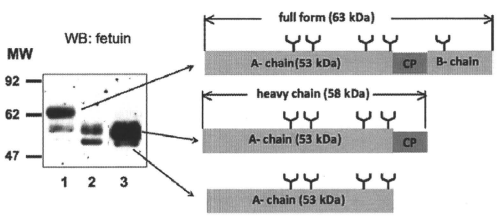

Figure 3. The molecular mass of fetuin in the high molecular fraction eluted on a Superdex column differed from fetuin in the low molecular fraction. The eluted fractions of the Superdex column (10 μl) were electrophoresed on a 10% SDS polyacrylamide gel under reducing conditions. Lane 1, high molecular fraction; lane 2, low molecular fraction; lane 3, total serum fetuin. High molecular fetuin was expected as a complete form of fetuin, which consists of an A-chain, a connecting peptide (CP) and a B-chain. The molecular mass of fetuin differed slightly between the high and low molecular fractions.

gel, confirmed by Western blot analysis (Fig. 5A), and visualized using silver staining (Fig. 5B). Co-purified molecules with fetuin were identified using mass spectro-metry. Major proteins identified by mass spectrometry are listed in Fig. 5C.

Lectin microarray. Since changes in oligosaccharide structures are linked to the susceptibility to certain cases of proteolysis, we analyzed the oligosaccharide structures on fetuin with a lectin microarray. While this system is limited to quantitation of the details of oligosaccharide structures, the array is capable of evaluating native oligosaccharides on glycoproteins. Increases in fucosylation and decreases in the sialylation of fetuin derived from sera of patients with pancreatic cancer were observed as expected (Fig. 6). The oligosaccharides of fetuin derived from sera of patients with pancreatic cancer showed a similar pattern to those in hepatoma cells.

Discussion

Although fetuin is an abundant protein in serum, its biological functions remain controversial despite the establishment of fetuin-deficient mice. Recently, fetuin levels were found to be increased in patients with non-alcoholic fatty liver disease (29), as well as in patients with arteriosclerotic calcifications (30). These investigations were performed due to previous reports that fetuin inhibited the reaction of insulin and TGF-β. However, fetuin levels were changed less than 2-fold in these diseases. Fetuin is well known as a negative acute reactant, while its levels are up- or down-regulated in chronic diseases, including cancer and metabolic syndrome.

The data suggest that the biological reaction of fetuin is dependent on the regulation of other molecules. Therefore, the question of how fetuin exists in serum is critical. Nawaratil *et al* reported limited proteolysis of fetuin by chymotrypsin treatment (6). This prompted us to perform the experiment described in Fig. 1. Notably, in 50% of the patients with pancreatic cancer, fetuin was resistant to chymotrypsin treatment. Other serum proteins, such as antitrypsin, haptoglobin and transferrin, showed no changes in proteolysis by chymotrypsin between pancreatic cancer patients and normal volunteers (data not shown), suggesting that the heterogeneity of fetuin but not the existence of protease inhibitors is a key factor in the resistance to chymotrypsin treatment.

These heterogeneities include glycosylation and complex formation. Gel filtration chromatography of sera from a patient with pancreatic cancer followed by ELISA showed small amounts of fetuin at a high molecular weight (Figs. 2 and 3). The data suggest that fetuin forms homo/hetero

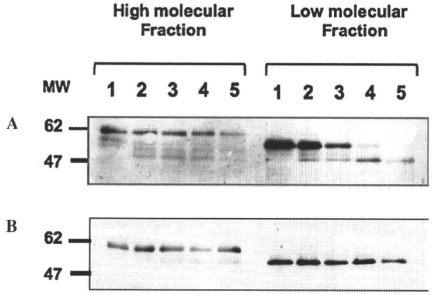

Figure 4. Fetuin in the high molecular fraction was resistant to treatment with chymotrypsin and trypsin. High and low molecular fractions eluted on a Superdex column were incubated with various concentrations of bovine pancreatic chymotrypsin for 30 min at 37˚C. (A) Chymotrypsin and (B) trypsin concentrations were each as follows: lane 1, 0 μg/μl; lane 2, 0.05 μg/μl, lane 3, 0.1 μg/μl; lane 4, 0.2 μg/μl, and lane 5, 0.5 μg/μl. Each sample was electrophoresed on a 10% SDS polyacrylamide gel, and then Western blot analysis was performed.

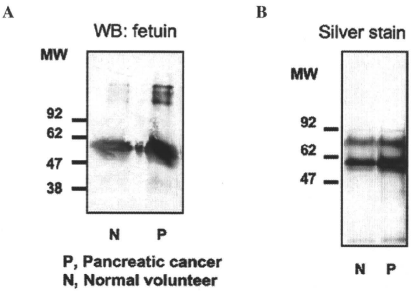

C

Normal & Pancreatic cancer	Pancreatic cancer
Centrosomal Protein 2	Ankyrin repeat domain protein21
Testis-specific Y-encoded-like protein 3	Protein C21 or rf
Ig Kappa chain C region	Haptoglobin
Zinc Finger Protein	Ig alpha-1 chain C region

Figure 5. Identification of fetuin-associated proteins. (A) Fetuin was purified from sera of patients with pancreatic cancer and normal volunteers using an anti-fetuin antibody affinity column, and confirmed by Western blot analysis. (B) Eluted proteins were visualized by silver stain. (C) Fetuin-associated proteins were identified by mass spectrometry. The results are described as common proteins for normal volunteers and pancreatic cancer patients, and as specific proteins for pancreatic cancer patients.

multivalent complexes. While it was unclear whether or not the complex formation of fetuin is involved in the resistance to chymotrypsin treatment, the molecular weight of fetuin differed between the complex and free forms of fetuin at 58 kDa in a Western blot analysis under reducing conditions. Fetuin at 65 kDa is a full form with an A chain, a connecting peptide and a B chain. While this form of fetuin was present at quite low levels, it was detected with mass spectrometry in normal sera (personal communication with Dr Yoshinao Wada, Osaka Medical Center and Research Institute for Maternal and Child Health, Japan).

Although the total levels of fetuin were decreased in patients with pancreatic cancer, a slight increase in the level of complex types of fetuin was observed (data not shown). However, this mass of fetuin was a minor fraction, possibly less than 1%. Haptoglobin was identified as a fetuin-binding protein using mass spectrometry analysis. This binding was also confirmed by co-purification experiments (data not shown). The binding capacity of fetuin with other serum proteins may reflect a resistance to various types of proteases. Notably, fetuin and haptoglobin are target proteins for fucosylation in cancer, since the level of fucosylated haptoglobin was increased in patients with pancreatic cancer (31) and fetuin was identified as a fucosylated protein in patients with hepatocellular carcinoma (32). A common lectin for fucosylated proteins might exist, which binds to fucosylated haptoglobin

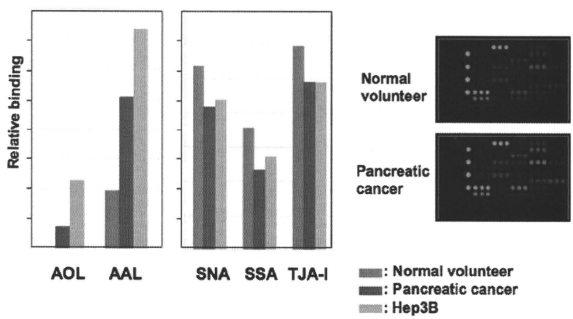

Figure 6. Lectin microarray analysis on fetuin derived from sera of patients with pancreatic cancer and from normal controls. Fetuin purified from sera of patients with pancreatic cancer (Group IV in Fig. 1) and normal volunteers and the conditioned medium of a human hepatoma cell line Hep3B were subjected to lectin microarray. AOL and AAL lectins recognized α1-3/α1-4/α1-6 fucosylation. SSA, SNA and TJA-I lectins recognized α2-6 sialylation. Fetuin derived from Hep3B served as a positive control for fucosylated fetuin.

and fetuin. Fucosylation itself might regulate proteolysis with chymotrypsin treatment.

While fetuin was found to have varying heterogeneity in serum, we did not find direct evidence for the variation in the resistance to protease digestion by fetuin molecules. Further studies are required to determine the relationship between the heterogeneity of fetuin and various diseases as well for the functional analysis of various types of fetuins.

Acknowledgements

This study was supported by a Grant-in-Aid for Scientific Research (A), No. 21249038, from the Japan Society for the Promotion of Science and the Global COE program of Osaka University funded by the Ministry of Education, Culture, Sports, Science and Technology of Japan, and the New Energy and Industrial Technology Development Organization (NEDO) as part of a developing-technology project for implementing sugar chain functions in Japan. We would like to thank Drs Naoyuki Taniguchi and Norihiko Nakano (Department of Biochemistry, Osaka University Graduate School of Medicine, Japan) for assisting in the preparation of the anti-fetuin antibody.

References

1. Dziegielewska KM, Brown WM, Casey SJ, Christie DL, Foreman RC, Hill RM, Saunders NR: The complete cDNA and amino acid sequence of bovine fetuin. J Biol Chem 265: 4354-4357, 1990.
2. Denecke B, Gräber S, Schäfer C, Heiss A, Wöltje M and Jahnen-Dechent W: Tissue distribution and activity testing suggest a similar but not identical function of fetuin-B and fetuin-A. Biochem J 376: 135-145, 2003.
3. Yoshioka Y, Gejyo F, Marti T, Rickli EE, Bürgi W, Offner GD, Troxler RF and Schmid K: The complete amino acid sequence of the A-chain of human plasma alpha 2 HS-glycoprotein. J Biol Chem 261: 1665-1676, 1986.
4. Gejyo F, Chang JL, Bürgi W, Schmid K, Offner GD, Troxler RF, van Halbeek H, Dorland L, Gerwig GJ and Vliegenthart JF: Characterization of the B-chain of human plasma alpha 2HS-glycoprotein. The complete amino acid sequence and primary structure of its heteroglycan. J Biol Chem 258: 4966-4971, 1983.
5. Kellermann J, Haupt H, Auerswald EA and Müller-Esterl W: The arrangement of disulfide loops in human alpha 2-HS glycoprotein. Similarity to the disulfide bridge structures of cystatins and kininogens. J Biol Chem 264: 14121-14128, 1989.
6. Nawratil P, Lenzen S, Kellermann J, Haupt H, Schinke T, Müller-Esterl W and Jahnen-Dechent W: Limited proteolysis of human α2-HS glycoprotein/fetuin. J Biol Chem 271: 31735-31741, 1996.
7. Hayase T, Rice KG, Dziegielewska KM, Kuhlenschmidt M, Reilly T and Lee YC: Comparison of N-glycosides of fetuins from different species and human alpha2-HS-glycoprotein. Biochemistry 31: 4915-4921, 1992.
8. Edge AS and Spiro RG. Presence of an O-glycosidically linked hexasaccharide in fetuin. J Biol Chem 262: 16135-16141, 1987.
9. Triffitt JT, Gebauer U, Ashton BA, Owen ME and Reynolds JJ: Origin of plasma α2HS-glycoprotein and its accumulation in bone. Nature 262: 226-227, 1976.
10. Ruminy P, Gangneux C, Claeyssens S, Scotte M, Daveau M and Salier JP: Gene transcription in hepatocytes during the acute phase of a systemic inflammation: from transcription factors to target genes. Inflamm Res 50: 383-390, 2001.
11. Szweras M, Liu D, Partridge EA, Pawling J, Sukhu B, Clokie C, Jahnen-Dechent W, Tenenbaum HC, Swallow CJ, Grynpas MD and Dennis JW: Alpha 2 HS glycoprotein, an antagonist of transforming growth factor beta in vivo, inhibits intestinal tumor progression. Cancer Res 64: 6402-6409, 2004.
12. Kalabay L, Jakab L, Prohászka Z, Füst G, Benkö Z, Telegdy L, Lörincz Z, Závodszky P, Arnaud P and Fekete B: Human fetuin/alpha 2 HS glycoprotein level as a novel indicator of liver cell function and short-term mortality in patients with liver cirrhosis and liver cancer. Eur J Gastroenterol Hepatol 14: 389-394, 2002.
13. Kishore BK, Gejyo F and Arakawa M: Alpha 2 HS-glycoprotein in the serum and urine of patients with renal diseases. Postgrad Med J 59: 304-307, 1983.
14. Schinke T, Amendt C, Trindl A, Pöschke O, Müller-Esterl W and Jahnen-Dechent W: The serum protein alpha2-HS glycoprotein/fetuin inhibits apatite formation in vitro and in mineralizing calvaria cells. J Biol Chem 271: 20789-20796, 1996.
15. Heiss A, DuChesne A, Denecke B, Grötzinger J, Yamamoto K, Renné T and Jahnen-Dechent W: Structural basis of calcification inhibition by alpha2-HS glycoprotein/fetuin-A. J Biol Chem 278: 13333-13341, 2003.
16. Price PA and Lim JE: The inhibition of calcium phosphate precipitation by fetuin is accompanied by the formation of a fetuin-mineral complex. J Biol Chem 278: 22144-22152, 2003.
17. Doherty TM, Fitzpatrick LA, Inoue D, Qiao JH, Fishbein MC, Detrano RC, Shah PK and Rajavashisth TB: Molecular, endocrine, and genetic mechanisms of arterial calcification. Endocr Rev 25: 629-672, 2004.
18. Auberger P, Falquerho L, Contreres JO, Pages G, Le Cam G, Rossi B and Le Cam A: Characterization of a natural inhibitor of the insulin receptor tyrosine kinase: cDNA cloning, purification, and anti-mitogenic activity. Cell 58: 631-640, 1989.
19. Rauth G, Poschke O, Fink E, Eulitz M, Tippmer S, Kellerer M, Häring HU, Nawratil P, Haasemann M and Jahnen-Dechent W: The nucleotide and partial amino acid sequences of rat fetuin. Identity with the natural tyrosine kinase inhibitor of the rat insulin receptor. Eur J Biochem 204: 523-529, 1992.
20. Srinivas PR, Wagner AS, Reddy LV, Deutsch DD, Leon MA, Goustin AS and Grunberger G: Serum alpha 2-HS-glycoprotein is an inhibitor of the human insulin receptor at the tyrosine kinase level. Mol Endocrinol 7: 1445-1455, 1993.
21. Mathews ST, Srinivas PR, Leon MA and Grunberger G: Bovine fetuin is an inhibitor of insulin receptor tyrosine kinase. Life Sci 61: 1583-1592, 1997.
22. Mathews ST, Chellam N, Srinivas PR, Cintron VJ, Leon MA, Goustin AS and Grunberger G: Alpha 2-HSG, a specific inhibitor of insulin receptor autophosphorylation, interacts with the insulin receptor. Mol Cell Endocrinol 164: 87-98, 2000.
23. Wang H, Zhang M, Soda K, Sama A and Tracey KJ: Fetuin protects the fetus from TNF. Lancet 350: 861-862, 1997.
24. Stefan N, Hennige AM, Staiger H, Machann J, Schick F, Kröber SM, Machicao F, Fritsche A and Häring HU: Alpha2-Heremans-Schmid glycoprotein/fetuin-A is associated with insulin resistance and fat accumulation in the liver in humans. Diabetes Care 29: 853-857, 2006.
25. Mori K, Emoto M, Yokoyama H, Araki T, Teramura M, Koyama H, Shoji T, Inaba M and Nishizawa Y: Association of serum fetuin-A with insulin resistance in type 2 diabetic and nondiabetic subjects. Diabetes Care 29: 468, 2006.
26. Jahnen-Dechent W, Schinke T, Trindl A, Müller-Esterl W, Sablitzky F, Kaiser S and Blessing M: Cloning and targeted deletion of the mouse fetuin gene. J Biol Chem 272: 31496-31503, 1997.
27. Schafer C, Heiss A, Schwarz A, Westenfeld R, Ketteler M, Floege J, Muller-Esterl W, Schinke T and Jahnen-Dechent W: The serum protein α2-Heremans-Schmid glycoprotein/fetuin-A is a systemically acting inhibitor of ectopic calcification. J Clin Invest 112: 357-366, 2003.
28. Kuno A, Uchiyama N, Koseki-Kuno S, Ebe Y, Takashima S, Yamada M and Hirabayashi J: Evanescent-field fluorescence-assisted lectin microarray: a new strategy for glycan profiling. Nat Methods 2: 851-856, 2005.
29. Reinehr T and Roth CL: Fetuin-A and its relation to metabolic syndrome and fatty liver disease in obese children before and after weight loss. J Clin Endocrinol Metab 93: 4479-4485, 2008.
30. Ix JH, Chertow GM, Shlipak MG, Brandenburg VM, Ketteler M and Whooley MA: Association of fetuin-A with mitral annular calcification and aortic stenosis among persons with coronary heart disease: data from the Heart and Soul Study. Circulation 115: 2533-2539, 2007.
31. Okuyama N, Ide Y, Nakano M, *et al*: Fucosylated haptoglobin is a novel marker for pancreatic cancer. Int J Cancer 118: 2803-2808, 2006.
32. Comunale MA, Lowman M, Long RE, Krakover J, Philip R, Seeholzer S, Evans AA, Hann HW, Block TM and Mehta AS: Proteomic analysis of serum associated fucosylated glycoproteins in the development of primary hepatocellular carcinoma. J Proteome Res 5: 308-315, 2006.

Cancer Science
The official journal of the Japanese Cancer Association

Contribution of BCR–ABL-independent activation of ERK1/2 to acquired imatinib resistance in K562 chronic myeloid leukemia cells

Takeru Nambu,[1] Norie Araki,[2,5] Aiko Nakagawa,[1] Akihiko Kuniyasu,[3] Tatsuya Kawaguchi,[4] Akinobu Hamada[1] and Hideyuki Saito[1,5]

[1]Department of Pharmacy, Kumamoto University Hospital, Kumamoto; [2]Department of Tumor Genetics and Biology, Graduate School of Medical Sciences, Kumamoto University School of Medicine, Kumamoto; [3]Department of Molecular Cell Function, Graduate School of Pharmaceutical Sciences, Kumamoto University, Kumamoto; [4]Department of Hematology and Infectious Diseases, Kumamoto University Hospital, Kumamoto, Japan

(Received July 3, 2009/Revised September 4, 2009/Accepted September 8, 2009/Online publication October 14, 2009)

BCR–ABL tyrosine kinase, generated from the reciprocal chromosomal translocation t(9;22), causes chronic myeloid leukemia (CML). BCR–ABL is inhibited by imatinib; however, several mechanisms of imatinib resistance have been proposed that account for loss of imatinib efficacy in patients with CML. Previously, we showed that overexpression of the efflux drug transporter P-glycoprotein partially contributed to imatinib resistance in imatinib-resistant K562 CML cells having no BCR–ABL mutations. To explain an additional mechanism of drug resistance, we established a subclone (K562/R) of the cells and examined the BCR–ABL signaling pathway in these and wild-type K562 (K562/W) cells. We found the K562/R cells were 15 times more resistant to imatinib than their wild-type counterparts. In both cell lines, BCR–ABL and its downstream signaling molecules, such as ERK1/2, ERK5, STAT5, and AKT, were phosphorylated in the absence of imatinib. In both cell lines, imatinib effectively reduced the phosphorylation of all the above, except ERK1/2, whose phosphorylation was, interestingly, only inhibited in the wild-type cells. We then observed that phospho-ERK1/2 levels decreased in the presence of siRNA targeting BCR–ABL, again, only in the K562/W cells. However, using an ERK1/2 inhibitor, U0126, we found that we could reduce phospho-ERK1/2 levels in K562/R cells and restore their sensitivity to imatinib. Taken together, we conclude that the BCR–ABL-independent activation of ERK1/2 contributes to imatinib resistance in K562/R cells, and that ERK1/2 could be a target for the treatment of CML patients whose imatinib resistance is due to this mechanism. (*Cancer Sci* 2010; 101: 137–142)

Chronic myeloid leukemia, a hematopoietic stem cell disorder, is characterized by the expression of the chimeric BCR–ABL oncoprotein, caused by the reciprocal chromosomal translocation t(9;22) (q34;q11), which generates a shortened chromosome 22 or Philadelphia chromosome.[1] BCR–ABL is a cytoplasmic protein with constitutive tyrosine kinase activity responsible for transformation and leukemogenic effects. BCR–ABL is the target of the tyrosine kinase inhibitor imatinib, which also inhibits c-kit protooncogene/CD117 (c-KIT) and plate-derived growth factor receptor (PDGFR).[2] More than 90% of chronic-phase CML patients respond to imatinib, at least initially, and a high percentage of them achieve cytogenic complete responses.[3] However, some patients fail to respond to treatment with imatinib in front-line therapy (primary resistance), while others stop responding after an initial response (acquired resistance).[4] Frequent clinical relevancies to imatinib resistance include point mutations in the *ABL* gene[5,6] and amplification of the *BCR–ABL* fusion gene.[7] In addition to these BCR–ABL-dependent mechanisms, BCR–ABL-independent mechanisms of imatinib resistance have been proposed, which involve the drug transporter P-gp (MDR1, ATP-binding cassette subfamily B1 (ABCB1)),[8–10] the drug carrier serum α_1 acid glycoprotein,[11] and signal cascades via LYN kinase.[12,13] Although some mechanisms of imatinib resistance are understood, resistance to this drug is still an important challenge confronting the effective treatment of CML.

We previously focused on drug transporters and reported the potential contribution to imatinib resistance of P-gp, a multidrug efflux transporter, using K562 cells, which are known as a representative human CML cell line.[9] In a previous study, we established imatinib-resistant K562 (prevK562/R) cells, which had wild-type BCR–ABL and overexpressed P-gp. In prevK562/R cells, intracellular imatinib levels were 42% less than those in wild-type K562 (K562/W) cells. Intracellular imatinib accumulation was restored completely by CysA, a P-gp inhibitor; however, CysA did not completely overcome prevK562/R cell sensitivity to imatinib. Therefore, we assumed that another mechanism was also involved in imatinib resistance in K562 cells. To identify this unknown mechanism, we focused on signal transduction pathways that were downstream of BCR–ABL, and analyzed imatinib resistance factors, other than overexpression of P-gp, using a new imatinib-resistant subclone of K562 (K562/R) cells, which was cloned from prevK562/R cells.

BCR–ABL has multiple downstream survival pathways, including ERK1/2, ERK5, AKT, JAK/STAT, nuclear factor kappa beta (NF-κB), and BCL-x_L.[14–18] Phosphorylation of tyrosine 177 of BCR–ABL is necessary for binding of the adaptor growth factor receptor-bound protein (GRB2) to BCR–ABL, which involves the recruitment of son of sevenless (SOS), the nucleotidic exchange factor of RAS.[19] RAS activates both the RAF–MEK–ERK1/2 and PI3K–AKT pathways, which are engaged in cell survival and anti-apoptosis.[18,20] ERK5, like ERK1/2, is a member of the mitogen-activated protein kinase family, is modulated by BCR–ABL, and contributes to the survival of leukemia cells.[17,21] In the present study, we investigated the contributions of these downstream factors to imatinib resistance in K562/R cells.

Here, we demonstrate that BCR–ABL-independent activation of ERK1/2 may contribute to imatinib resistance in certain CML cell lines. This resistance can be overcome by co-treatment with the specific ERK1/2 inhibitor and imatinib, indicating that this co-treatment may be effective for imatinib-resistant CML patients.

Materials and Methods

Cell culture and cloning of imatinib-resistant K562 cells. K562/W cells were cultured in RPMI-1640 medium supplemented with

[5]To whom correspondence should be addressed.
E-mail: saitohide@fc.kuh.kumamoto-u.ac.jp; nori@gpo.kumamoto-u.ac.jp

doi: 10.1111/j.1349-7006.2009.01365.x

10% FBS under an atmosphere of 5% CO_2–95% air at 37°C. prevK562/R cells were established by exposing gradually increasing concentrations of imatinib (from 0.3 to 10 μM) from K562/W cells.[9] The new clonal cell line K562/R was established by limiting dilution from prevK562/R cells. K562/R cells were maintained under the same culture conditions in the presence of 1 μM imatinib.

mRNA isolation and cDNA synthesis. For mRNA extraction, MagNA Pure LC mRNA Isolation Kit II (Roche Diagnostics, Basel, Switzerland) was used as per the instruction manual. cDNA was synthesized by reverse transcription using the High-Capacity cDNA Archive Kit (Applied Biosystems, Foster City, CA, USA). Each prepared cellular cDNA was stored at –30°C.

Mutation analysis of the *BCR–ABL* kinase domain and *KRAS*. The kinase domain of *BCR–ABL* was amplified by PCR using each cellular cDNA.[9] For the primary PCR, we used the forward primer 5′-CCAGACTGTCCACAGCATTC-3′ and the reverse primer 5′-ATGGTCCAGAGGATCGCTCTCT-3′, and for the secondary PCR, the forward primer 5′-GGGAGGGTGTACCATTACAGG-3′ and the reverse primer, 5′-GCTGTGTAGGTGTCCCCTGT-3′, or the forward primer 5′-CCACTTGGTGAAGGTAGCTG-3′ and the reverse primer, 5′-CCTGCAGCAAGGTAGTCACA-3′, were used. The analysis was carried out by DNA sequencing using an Applied Biosystems 3130 Genetic Analyzer. For the mutation analysis of *KRAS ORF*, the forward primer 5′-CGGGAGAGAGGCCTGCTG-3′ and the reverse primer 5′-CCACTTGTACTAGTATGCCT-3′ were used in PCR amplification. The sequence of the *KRAS* gene was analyzed by the Sigma-Aldrich DNA sequencing Service.

Cytotoxicity assay. The individual or combined cytotoxicities of imatinib and U0126 were determined by the Alamar Blue assay as described previously.[9,22] Absorbance in cells without drug treatment was 100%.

Western blot analysis. K562/W and K562/R cells were homogenized in a solution containing 7 M urea, 2 M thiourea, 4% CHAPS, protease inhibitor cocktail (P8430; Sigma-Aldrich, St Louis, MO, USA), 2 mM Na_3VO_4, 10 mM NaF, 1 μM okadaic acid, and 1 mM DTT, using Micropestle (Eppendorf, Westbury, NY, USA). Crude membrane fraction selection and Western blotting conditions were as described previously.[9] The following primary antibodies were used: LYN, phospho-STAT5 (Tyr^{694}), STAT5 (BD Transduction Laboratories, Lexington, KY, USA), β-actin (Sigma-Aldrich), 4G10, Na^+/K^+ ATPase α-1 (Upstate Biotechnology, Lake Placid, NY, USA), c-ABL (Santa Cruz Biotechnology, Santa Cruz, CA, USA), phospho-ERK1/2, ERK1/2, phospho-AKT (Thr^{308}), phospho-AKT (Ser^{473}), AKT, ERK5 (Cell Signaling Technology, Beverly, MA, USA), and P-gp (C219 monoclonal antibody; Signet Laboratories, Dedham, MA, USA).

Two-dimensional Western blotting. Samples were desalted using the 2-D Clean-Up kit (GE Healthcare, Amersham Place, UK) and resolved with sample buffer (7 M urea, 2 M thiourea, 4% CHAPS, 0.5% IPG Buffer pH 3–10, and Destreaking buffer). The first-dimensional isoelectric focusing (pH 3–10, 7 cm) was carried out using the Ettan IPGPhor Cup Loading Manifold electrophoresis system (GE Healthcare) as per manufacturer recommendations. After reduction and alkylation of disulfide bonds with 10 mg/mL DTT and 25 mg/mL iodoacetamide, respectively, the second-dimensional separation was carried out by 12% SDS-PAGE. The 2D gel was immunoblotted as indicated above.

Real-time RT-PCR analysis. To determine the expression levels of *hMDR1* and *hβ-ACTIN* in the cells, we carried out TaqMan quantitative real-time RT-PCR using the ABI PRISM 7900 sequence detection system (Applied Biosystems), using the manufacturer's standard protocol (*hMDR1*, Hs00184491_m1; *hβ-ACTIN*, 4310881E).

Analysis of intracellular imatinib accumulation. Cells (2×10^6) were incubated in 5 mL incubation buffer (150 mM NaCl, 3 mM KCl, 1 mM $CaCl_2$, 0.5 mM $MgCl_2$, 5 mM D-glucose, 5 mM HEPES, pH 7.4) containing 1 μM imatinib. The cell pellet was washed once in ice-cold PBS containing 1% BSA, and twice with ice-cold PBS. The cellular imatinib was then extracted by incubation with 300 μL of 50% methanol (HPLC mobile phase/methanol = 1/1) for 30 min. Quantification of imatinib was done using the HPLC (model LC-6A; Shimadzu, Kyoto, Japan) method described previously.[8] For the cellular protein quantitation, the pellet was solubilized with 200 μL of 1 N NaOH and analyzed by the Bradford method, using a Bio Rad Protein Assay kit (Bio Rad, Hercules, CA, USA) with BSA as a standard.

siRNA transfection. An siRNA specific for the b3a2 breakpoint of the *BCR–ABL* gene (5′-GCAGAGUUCAAAAGCCCUUdTdT), and a control siRNA composed of the scrambled b3a2 sequence (5′-GCAGAGUUCUAAAGCGCUUdTdT),[23] were synthesized by Nippon EGT (Toyama, Japan). For electroporation of K562/W and K562/R cells, we used Micro-Porator MP-100 (AR Brown, Tokyo, Japan). Cells were washed twice with PBS, and mixed with 20 μM stock siRNA to a final concentration of 3, 4 or 8 pmol/μL. Subsequently, 5×10^5 cells/10 μL of the cell suspension were electroporated using the following settings: pulse voltage = 1450 V, pulse width = 10 ms, and pulse number = three times. After electroporation, the cells were resuspended in RPMI-1640 medium and cultured in the incubator for 48 h under the same conditions as other cells.

Statistical analysis. Statistical significance was determined by Welch's *t*-test. $P < 0.05$ was considered statistically significant.

Results

Characterization of imatinib-resistant K562/R cells. We established a new K562/R clonal cell line, which indicated a 15-fold increase in the IC_{50} of imatinib over the parent K562/W cells (Fig. 1A), had no mutation in the BCR–ABL kinase domain (data not shown), and had neither overexpression nor overactivation of BCR–ABL or LYN kinase (Fig. 1B). Mutation analysis of *KRAS* showed no missense mutations[24,25] in either cell line, although one silent mutation (519T > C) was found in both cells (Supporting information Fig. S1), suggesting that *KRAS* mutation in K562/R cells is not a factor in imatinib resistance. Both levels of mRNA (300-fold, $P < 0.01$; Fig. 1C) and protein in the crude membrane fraction (Supporting information Fig. S2B) of MDR1 were found to be elevated in K562/R cells compared with K562/W cells (almost similar results were obtained in prevK562/R cells[9]), although intracellular accumulation levels of imatinib were similar (Fig. 1D). Moreover, CysA, a P-gp inhibitor, did not influence intracellular imatinib accumulation levels in either type of cell. These results suggest that the imatinib resistance of K562/R cells is not directly related to the cellular P-gp expression level or function.

Imatinib did not inhibit the phosphorylation of ERK1/2 in K562/R cells. To study the specific activation signals in K562/R cells, K562/W and K562/R cells were treated with imatinib for varying lengths of time, as shown in Figure 2(A), after which the phosphorylation of BCR–ABL and its downstream factors, AKT, ERK5, STAT5, and ERK1/2 was examined. The phosphorylation levels of BCR–ABL and STAT5 were similarly high in both cell lines, but those of AKT and ERK1/2 were higher in the K562/R cells. After the treatment with imatinib, the phosphorylation of BCR–ABL, AKT, and STAT5 was effectively inhibited in both cell lines (Fig. 2A). ERK5 expression, which is known to be regulated by BCR–ABL,[17] was not decreased by imatinib in either cell line (Fig. 2A). To analyze the phosphorylation status of ERK5 in both cell lines, we carried out 2D Western blotting using anti-ERK5 antibodies after a 24-h treatment

doi: 10.1111/j.1349-7006.2009.01365.x

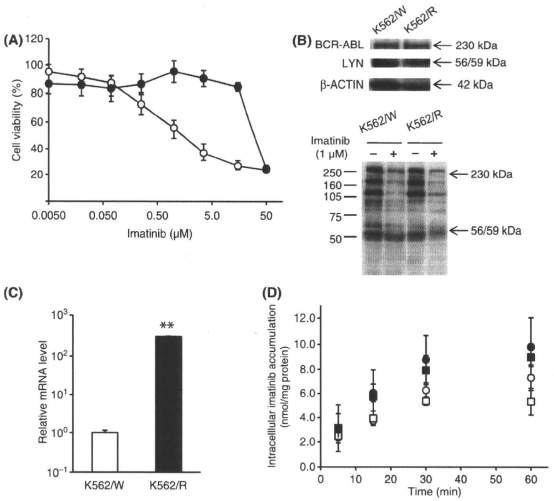

Fig. 1. Characteristics of imatinib-resistant K562/R cells. Imatinib and FBS were depleted from the medium 1 day before all experimental procedures to efflux intracellular imatinib from K562/R cells. (A) K562/W (open circles) and K562/R (closed circles) cells were exposed to various concentrations of imatinib for 48 h. Cell viability was assayed by Alamar Blue. Each point represents the mean ± SD from six cells. (B) The expression levels of BCR–ABL, LYN, and β-actin and phosphorylation of tyrosine were examined by Western blot analysis. K562/W and K562/R cells were treated with 1 μM imatinib for 15 min. (C) The mRNA levels of *hMDR1* and *hβ-ACTIN* were examined by real time RT-PCR analysis. The relative amount of *hMDR1* mRNA was normalized to that of *hβ-ACTIN*. (D) Intracellular imatinib accumulation was measured by HPLC analysis in K562/W and K562/R cells. The cells (2.0×10^6) were exposed to 1 μM imatinib with (squares) or without (circles) 5 μM cyclosporin A (CysA) at 37°C for varying lengths of time in K562/W (open symbols) and K562/R (closed symbols). Each point represents the mean ± SD from four cells. $^{**}P < 0.01$ *versus* K562/W cells.

with imatinib, and compared the 2D patterns of ERK5-positive spots (Fig. 2C). Prior to imatinib treatment, both cell lines showed at least two ERK5-positive spots in 2D Western blotting. After treatment, one of these spots, presumed to be phosphorylated ERK5, underwent a significant shift from left (acid, pI 4.7) to right (basic, pI 4.9), suggesting that the phosphorylation of ERK5 was inhibited by the imatinib treatment in both cell lines. In contrast, ERK1/2 phosphorylation was inhibited in K562/W cells only (Fig. 2A). Interestingly, imatinib inhibitory effects on the phosphorylation of BCR–ABL were significant in a dose-dependent manner, while phosphorylation of ERK1/2 was never downregulated by imatinib in K562/R cells (Fig. 2B). Results similar to the above were obtained in prevK562/R cells (Supporting information Fig. S2A) and eight other clones also established as imatinib-resistant K562 cells (Fig. 2D). These results strongly indicate that, unlike in K562/W cells, BCR–ABL does not play a major role in the phosphorylation of ERK1/2 in K562/R cells.

BCR–ABL-targeting siRNA decreased the phosphorylation of ERK1/2 in K562/W cells, but not in K562/R cells. To confirm that ERK1/2 was activated independently of BCR–ABL in K562/R cells, BCR–ABL-targeting siRNA was transfected into cells from both cell lines. Since K562 cells express the b3a2 form of the BCR–ABL fusion mRNA, the specific sequence for b3a2 can effectively silence cellular BCR–ABL expression.[23] Transient transfection with varying amounts of b3a2 BCR–ABL siRNA significantly reduced the expression of BCR–ABL protein but not that of c-ABL in K562/W cells, compared with cells transfected with a control scrambled siRNA (Fig. 3A). The same treatment also induced the downregulation of phosphorylated-ERK1/2 in K562/W cells; however, it did not have this effect on K562/R cells (Fig. 3B).

Inhibition of ERK1/2 overcame imatinib resistance in K562/R cells. Because the results obtained from the above experiments strongly suggested that the BCR–ABL-independent activation of ERK1/2 is directly related to the mechanism of imatinib resistance in K562/R cells, we examined the effect of ERK1/2 inhibition on these cells. Treatment with an ERK1/2 inhibitor, U0126,[26] alone for 48 h showed similar dose-dependent toxicity for K562/W and K562/R cells (Fig. 4A). Treatment with U0126 (1 μM) alone had little cytotoxic effect on either cells; however, in combination with imatinib, cell death increased dramatically, with both cells showing a similar sensitivity to imatinib (Fig. 4B). These results suggest that co-administration of the ERK1/2 inhibitor with imatinib could overcome imatinib resistance in K562/R cells.

Co-treatment of imatinib and U0126 inhibited phosphorylation of ERK1/2 in both K562/W and K562/R cells. Because co-administration of imatinib with U0126 restored imatinib sensitivity in K562/R cells, we next analyzed the inhibitory effect of imatinib on ERK1/2 phosphorylation by Western blotting in both cell lines exposed to U0126 alone or combined with imatinib. After U0126 treatment for 24 h, a dose-dependent downregulation of ERK1/2 phosphorylation in both cell lines was observed (Fig. 5). Interestingly, co-administration of 1 μM imatinib with 1 μM U0126 remarkably inhibited the phosphorylation of ERK1/2 in K562/R cells. These results confirm that the BCR–ABL-independent ERK1/2 activation is essential for imatinib resistance in K562/R cells.

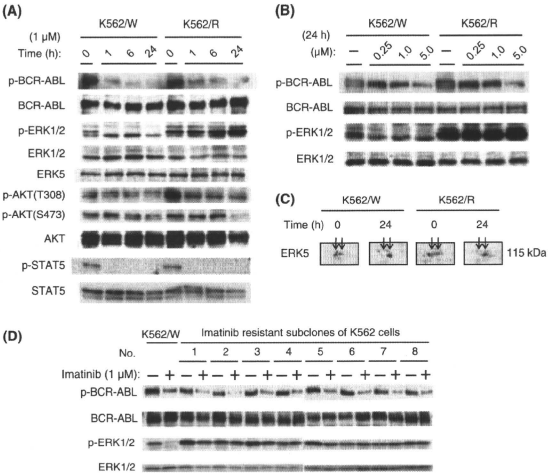

Fig. 2. Effects of imatinib on K562/W and K562/R cells were analyzed by immunoblotting. (A) Time course of BCR–ABL, ERK1/2, AKT, and STAT5 phosphorylation levels in K562/W and K562/R cells after 1 μM imatinib treatment. (B) Effect of the indicated concentrations of imatinib treatment for 24 h on the phosphorylation levels of BCR–ABL and ERK1/2 in K562/W and K562/R cells. (C) K562/W and K562/R cells were treated with 1 μM imatinib for 24 h. ERK5 was detected by 2D Western blotting. (D) K562/W and subcloned, imatinib-resistant K562 cells (from 1 to 8) were treated with 1 μM imatinib for 15 min. Clone cells of no. 2 is K562/R cells.

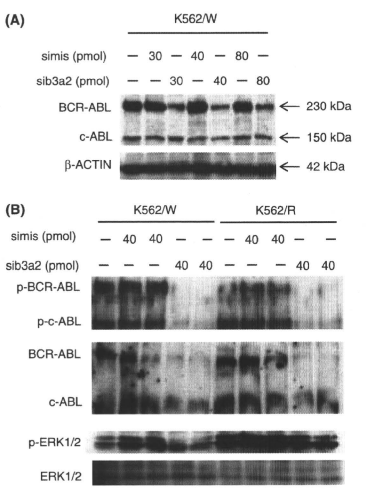

Fig. 3. Effects of BCR–ABL targeting siRNA on K562/W and K562/R cells. (A) K562/W cells were electroporated with different amounts of siRNA ranging from 30 to 80 pmol per 5×10^5 cells. (B) Effect of 40 pmol siRNA on the phosphorylation levels of BCR–ABL and ERK1/2 in K562/W and K562/R cells. sib3a2 and simis indicate BCR-ABL-specific siRNA and mismatch control siRNA, respectively.

Discussion

Despite the significant efficacy of imatinib in treating CML, the development of primary and acquired imatinib resistance is a problem in patients with CML. We previously reported that, although P-gp partly contributes to imatinib resistance in prevK562/R cells, P-gp function alone cannot fully explain the resistance to imatinib. We thus postulated the involvement of a separate mechanism, and established a new imatinib-resistant K562 clonal cell line (K562/R) from prevK562/R cells for use in studying this mechanism. In the new clonal cells, BCR–ABL was inhibited by both imatinib and BCR–ABL siRNA, while neither treatment suppressed ERK1/2 phosphorylation. Co-treatment with imatinib and the ERK1/2 inhibitor U0126 restored imatinib sensitivity in K562/R cells. These data suggested for the first time that ERK1/2, activated through a BCR–ABL-independent pathway, contributes to imatinib resistance in K562 cells.

Imatinib resistance is most often caused by BCR–ABL-dependent mechanisms, including point mutations in the functional kinase domain of BCR–ABL[5,6] and amplification of the *BCR–ABL* fusion gene.[7] Point mutations in *BCR–ABL* reduce the binding of imatinib to the protein by either a direct or an indirect mechanism. However, in our study, the K562/R cells showed neither *BCR–ABL* mutations nor overexpression (Fig. 1B), indicating that their imatinib resistance mechanism could involve a BCR–ABL-independent pathway. Similar mechanisms have been reported, namely, the overexpression of P-gp and LYN kinase.[10–13] Constitutively active mutants of KRAS are also known to be related to drug resistance in several cancers, including CML.[24,25,27–29] For example, mutations in *KRAS* codon 12 involving a substitution of valine for glycine or aspartic acid are known; however, these were not observed in our K562/W or K562/R cells. Although both cell lines had the 519T > C silent mutation at the translated region (Supporting information Fig. S1), this particular mutation would not seem to influence the sensitivity to imatinib. In addition, LYN, which is a member of the Src tyrosine kinase family and is reported to be involved in imatinib resistance through overexpression of the anti-apoptotic protein BCL-2,[12,13] is neither overexpressed nor overactivated in K562/R cells (Fig. 1B).

It is well known that imatinib interacts with P-gp as a substrate, and that overexpressed P-gp inhibits intracellular accumulation of imatinib.[8–10] In our study, although MDR1 mRNA and protein expression were higher in K562/R than K562/W

doi: 10.1111/j.1349-7006.2009.01365.x

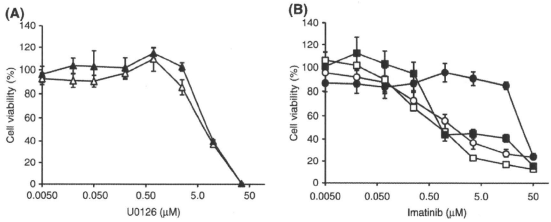

Fig. 4. Cytotoxicity of U0126 alone and cotreatment with imatinib in K562/W and K562/R cells. (A) K562/W (open triangles) and K562/R (closed triangles) cells were exposed to 0.0050 μM U0126 alone for 48 h. (B) K562/W (open symbols) and K562/R (closed symbols) cells were exposed to 0.0050–50 μM imatinib with (squares) or without (circles) 1 μM U0126 for 48 h. Cell viability was assayed by Alamar Blue. Each point represents the mean ± SD from six cells.

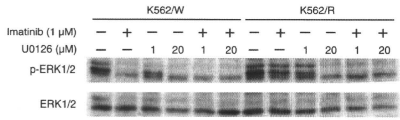

Fig. 5. The effects of imatinib and U0126, alone or in combination, on ERK1/2 phosphorylation. K562/W and K562/R cells were treated with or without 1 μM imatinib and U0126 (1 and 20 μM) for 24 h, as indicated.

cells, there was no difference in intracellular imatinib accumulation, which was not decreased by the P-gp inhibitor CysA (Fig. 1C,D). From these results, we hypothesized that P-gp functional activity was modulated by unknown factors in K562/R cells. Intracellular imatinib levels are possibly controlled by many factors, such as drug transporters and plasma carrier proteins, *in vivo*. Even though upregulation of MDR1 mRNA or protein is observed in imatinib-resistant CML patients, it will be necessary to measure intracellular imatinib levels to understand individual cases of imatinib resistance. Therefore, we ruled out a contribution from known mechanisms including P-gp, and postulated the involvement of a separate mechanism.

BCR–ABL has multiple downstream survival pathways, such as ERK1/2, ERK5, AKT, and JAK/STAT.[14–17] We examined whether imatinib treatment inhibited these downstream factors and found that the phosphorylation of BCR–ABL, ERK5, AKT, and STAT5 was indeed downregulated in both K562/W and K562/R cells, whereas ERK1/2 was not inhibited by imatinib in K562/R cells (Fig. 2A,C). A similar result was obtained by treatment using BCR–ABL siRNA (Fig. 3B), which further indicated that ERK1/2 is phosphorylated by a BCR–ABL-independent mechanism in the K562/R cells. Next, the contribution of ERK1/2 to imatinib resistance in the K562/R cells was examined (Figs 4,5). Although the cells were not sensitive to treatment with 1 μM imatinib alone, co-administration with 1 μM U0126 inhibited ERK1/2 phosphorylation and dramatically induced K562/R cell death. U0126 is a known inhibitor of ERK5 as well,[30] but because imatinib inhibited ERK5 phosphorylation (Fig. 2C), most of the synergistic effect of U0126 was presumably mediated by its downregulation of ERK1/2, rather than ERK5. These results demonstrate that inhibition of not only BCR–ABL, but also ERK1/2, due to its activation being independent of the former, is necessary to overcome imatinib resistance in the K562/R cells.

Concerning ERK1/2 activation in K562/R cells, the factors responsible have not been determined. It is known, however, that U0126 inhibits ERK1/2 through MEK1/2, which may be directly upstream of ERK1/2 in this BCR–ABL-independent pathway. We have also shown that the aberrant activation of LYN or KRAS is not involved (Fig. 1B; Supporting Information Fig. S1). However, the possibility remains that unknown factors could increase ERK1/2 sensitivity and activate this signal via weak activation of BCR–ABL.

Recently, new drugs have been developed to target the BCR–ABL-dependent and -independent imatinib-resistance mechanisms. Nilotinib and dasatinib have a greater affinity for BCR–ABL than imatinib, and inhibit BCR–ABL and Src kinase, respectively.[31,32] U0126 co-treatment with dasatinib reverses LYN-dependent imatinib resistance,[33] suggesting the efficacy of its combination with molecular target drugs. Sorafenib, which inhibits multiple kinases, induces apoptosis in both BCR–ABL-expressing imatinib-sensitive and -resistant cells.[34–36] It is possible that the combination of sorafenib with a BCR–ABL inhibitor works by inhibiting ERK1/2 activation in K562/R cells.

In conclusion, we demonstrate that ERK1/2, activated through a BCR–ABL-independent mechanism, contributes to imatinib resistance in certain CML cells (Supporting Information Fig. S3). Although further work is required to confirm whether or not this resistance mechanism occurs in patients with CML, our study shows that this mechanism can be overcome by inhibiting the ERK1/2 signaling pathway with specific drugs that could be candidates for targeting the CML cells resistant to imatinib.

Acknowledgments

This work was supported in part by a Grant-in-Aid for Scientific Research from the Japan Society for the Promotion of Science (JSPS) for Hideyuki Saito (KAKENHI 21390048) and Akinobu Hamada (KAKENHI 19590149) and from Cancer Research, Kiban Research, Houga Research from the Ministry of Education, Science, and Culture of Japan for Norie Araki (KAKENHI 17015034, 19390482, and 20659223, respectively). We thank Anthony Wilson, of the Tumor Genetics and Biology Department at Kumamoto University, for assistance with the English language presentation of this manuscript.

Disclosure Statement

None.

Abbreviations

ABL	Abelson
AKT	v-akt murine thymoma viral oncogene homolog
BCL	B-cell CLL/lymphoma 2
BCR	breakpoint cluster region
CML	chronic myeloid leukemia
CysA	cyclosporin A
LYN	v-yes-1 Yamaguchi sarcoma viral related oncogene homolog
P-gp	P-glycoprotein
PI3K	phosphoinositide 3-kinase
RAF	v-raf murine sarcoma viral oncogene homolog
RAS	rat sarcoma oncogene
STAT	signal transducer and activator of transcription

References

1 Kalidas M, Kantarjian H, Talpaz M. Chronic myelogenous leukemia. *JAMA* 2001; **286**: 895–8.
2 Capdeville R, Buchdunger E, Zimmermann J, Matter A. Glivec (STI571, imatinib), a rationally developed, targeted anticancer drug. *Nat Rev Drug Discov* 2002; **1**: 493–502.
3 Druker BJ, Guilhot F, O'Brien SG *et al.* Five-year follow-up of patients receiving imatinib for chronic myeloid leukemia. *N Engl J Med* 2006; **355**: 2408–17.
4 Daley GQ. Dodging the magic bullet: understanding imatinib resistance. *Cancer Biol Ther* 2003; **2**: 109–10.
5 Branford S, Rudzki Z, Walsh S *et al.* High frequency of point mutations clustered within the adenosine triphosphate-binding region of BCR/ABL in patients with chronic myeloid leukemia or Ph-positive acute lymphoblastic leukemia who develop imatinib (STI571) resistance. *Blood* 2002; **99**: 3472–5.
6 Roche-Lestienne C, Soenen-Cornu V, Grardel-Duflos N *et al.* Several types of mutations of the Abl gene can be found in chronic myeloid leukemia patients resistant to STI571, and they can pre-exist to the onset of treatment. *Blood* 2002; **100**: 1014–8.
7 Gorre ME, Mohammed M, Ellwood K *et al.* Clinical resistance to STI-571 cancer therapy caused by BCR–ABL gene mutation or amplification. *Science* 2001; **293**: 876–80.
8 Hamada A, Miyano H, Watanabe H, Saito H. Interaction of imatinib mesilate with human P-glycoprotein. *J Pharmacol Exp Ther* 2003; **307**: 824–8.
9 Hirayama C, Watanabe H, Nakashima R *et al.* Constitutive overexpression of P-glycoprotein, rather than breast cancer resistance protein or organic cation transporter 1, contributes to acquisition of imatinib-resistance in K562 cells. *Pharm Res* 2008; **25**: 827–35.
10 Mahon FX, Belloc F, Lagarde V *et al.* MDR1 gene overexpression confers resistance to imatinib mesylate in leukemia cell line models. *Blood* 2003; **101**: 2368–73.
11 Gambacorti-Passerini C, Barni R, le Coutre P *et al.* Role of alpha1 acid glycoprotein in the *in vivo* resistance of human BCR–ABL(+) leukemic cells to the abl inhibitor STI571. *J Natl Cancer Inst* 2000; **92**: 1641–50.
12 Donato NJ, Wu JY, Stapley J *et al.* BCR–ABL independence and LYN kinase overexpression in chronic myelogenous leukemia cells selected for resistance to STI571. *Blood* 2003; **101**: 690–8.
13 Dai Y, Rahmani M, Corey SJ, Dent P, Grant S. A Bcr/Abl-independent, Lyn-dependent form of imatinib mesylate (STI-571) resistance is associated with altered expression of Bcl-2. *J Biol Chem* 2004; **279**: 34227–39.
14 Jin A, Kurosu T, Tsuji K *et al.* BCR/ABL and IL-3 activate Rap1 to stimulate the B-Raf/MEK/Erk and Akt signaling pathways and to regulate proliferation, apoptosis, and adhesion. *Oncogene* 2006; **25**: 4332–40.
15 Sonoyama J, Matsumura I, Ezoe S *et al.* Functional cooperation among Ras, STAT5, and phosphatidylinositol 3-kinase is required for full oncogenic activities of BCR/ABL in K562 cells. *J Biol Chem* 2002; **277**: 8076–82.
16 Kirchner D, Duyster J, Ottmann O, Schmid RM, Bergmann L, Munzert G. Mechanisms of BCR–ABL-mediated NF-kappaB/Rel activation. *Exp Hematol* 2003; **31**: 504–11.
17 Buschbeck M, Hofbauer S, Di Croce L, Keri G, Ullrich A. Abl-kinase-sensitive levels of ERK5 and its intrinsic basal activity contribute to leukaemia cell survival. *EMBO Rep* 2005; **6**: 63–9.
18 Quintas-Cardama A, Cortes J. Molecular biology of BCR–ABL1-positive chronic myeloid leukemia. *Blood* 2009; **113**: 1619–30.
19 Pendergast AM, Quilliam LA, Cripe LD *et al.* BCR–ABL-induced oncogenesis is mediated by direct interaction with the SH2 domain of the GRB-2 adaptor protein. *Cell* 1993; **75**: 175–85.
20 McCubrey JA, Steelman LS, Abrams SL *et al.* Roles of the RAF/MEK/ERK and PI3K/PTEN/AKT pathways in malignant transformation and drug resistance. *Adv Enzyme Regul* 2006; **46**: 249–79.
21 Nishimoto S, Nishida E. MAPK signalling: ERK5 versus ERK1/2. *EMBO Rep* 2006; **7**: 782–6.
22 O'Brien J, Wilson I, Orton T, Pognan F. Investigation of the Alamar Blue (resazurin) fluorescent dye for the assessment of mammalian cell cytotoxicity. *Eur J Biochem* 2000; **267**: 5421–6.
23 Brauer KM, Werth D, von Schwarzenberg K *et al.* BCR–ABL activity is critical for the immunogenicity of chronic myelogenous leukemia cells. *Cancer Res* 2007; **67**: 5489–97.
24 Pao W, Wang TY, Riely GJ *et al.* KRAS mutations and primary resistance of lung adenocarcinomas to gefitinib or erlotinib. *PLoS Med* 2005; **2**: e17.
25 Agarwal A, Eide CA, Harlow A *et al.* An activating KRAS mutation in imatinib-resistant chronic myeloid leukemia. *Leukemia* 2008; **22**: 2269–72.
26 Bain J, McLauchlan H, Elliott M, Cohen P. The specificities of protein kinase inhibitors: an update. *Biochem J* 2003; **371**: 199–204.
27 Garnett MJ, Marais R. Guilty as charged: B-RAF is a human oncogene. *Cancer Cell* 2004; **6**: 313–9.
28 Weinstein-Oppenheimer CR, Henriquez-Roldan CF, Davis JM *et al.* Role of the Raf signal transduction cascade in the *in vitro* resistance to the anticancer drug doxorubicin. *Clin Cancer Res* 2001; **7**: 2898–907.
29 Davis JM, Navolanic PM, Weinstein-Oppenheimer CR *et al.* Raf-1 and Bcl-2 induce distinct and common pathways that contribute to breast cancer drug resistance. *Clin Cancer Res* 2003; **9**: 1161–70.
30 Kamakura S, Moriguchi T, Nishida E. Activation of the protein kinase ERK5/BMK1 by receptor tyrosine kinases. Identification and characterization of a signaling pathway to the nucleus. *J Biol Chem* 1999; **274**: 26563–71.
31 Kantarjian H, Giles F, Wunderle L *et al.* Nilotinib in imatinib-resistant CML and Philadelphia chromosome-positive ALL. *N Engl J Med* 2006; **354**: 2542–51.
32 Talpaz M, Shah NP, Kantarjian H *et al.* Dasatinib in imatinib-resistant Philadelphia chromosome-positive leukemias. *N Engl J Med* 2006; **354**: 2531–41.
33 Nguyen TK, Rahmani M, Harada H, Dent P, Grant S. MEK1/2 inhibitors sensitize Bcr/Abl+ human leukemia cells to the dual Abl/Src inhibitor BMS-354/825. *Blood* 2007; **109**: 4006–15.
34 Wilhelm SM, Carter C, Tang L *et al.* BAY 43-9006 exhibits broad spectrum oral antitumor activity and targets the RAF/MEK/ERK pathway and receptor tyrosine kinases involved in tumor progression and angiogenesis. *Cancer Res* 2004; **64**: 7099–109.
35 Rahmani M, Nguyen TK, Dent P, Grant S. The multikinase inhibitor sorafenib induces apoptosis in highly imatinib mesylate-resistant bcr/abl+ human leukemia cells in association with signal transducer and activator of transcription 5 inhibition and myeloid cell leukemia-1 down-regulation. *Mol Pharmacol* 2007; **72**: 788–95.
36 Kurosu T, Ohki M, Wu N, Kagechika H, Miura O. Sorafenib induces apoptosis specifically in cells expressing BCR/ABL by inhibiting its kinase activity to activate the intrinsic mitochondrial pathway. *Cancer Res* 2009; **69**: 3927–36.

Supporting Information

Additional Supporting Information may be found in the online version of this article:

Fig. S1. Mutation analysis of KRAS in (A) K562/W and (B) K562/R cells. The T519C silent mutation was observed in both cell lines.

Fig. S2. (A) Expression of P-glycoprotein in crude membrane fractions of K562/W, K562/R, and prevK562/R cells. (B) Effects of imatinib treatment on the phosphorylation levels of ERK1/2 in K562/W, K562/R, and prevK562/R cells. Cells were treated with the indicated concentrations of imatinib for 24 h, and phosphorylation levels were analyzed by Western blotting.

Fig. S3. Scheme of a BCR–ABL-independent imatinib-resistant mechanism in K562/R cells. In K562/R cells, ERK1/2 is activated by a BCR–ABL-independent pathway. Imatinib inhibits BCR–ABL and decreases phosphorylated AKT, but not phosphorylated ERK1/2, which is activated by an unknown protein independent of BCR–ABL.

Please note: Wiley-Blackwell are not responsible for the content or functionality of any supporting materials supplied by the authors. Any queries (other than missing material) should be directed to the corresponding author for the article.

doi: 10.1111/j.1349-7006.2009.01365.x

Original Article

A Novel Serum Carbohydrate Marker on Mucin 5AC

Values for Diagnostic and Prognostic Indicators for Cholangiocarcinoma

Atit Silsirivanit, PhD[1,2]; Norie Araki, PhD[3]; Chaisiri Wongkham, MD PhD[1,2]; Chawalit Pairojkul, MD[2,4]; Yoshiki Narimatsu, PhD[5]; Kazuhiko Kuwahara, MD, PhD[6]; Hisashi Narimatsu, MD, PhD[5]; Sopit Wongkham, PhD[1,2]; and Nobuo Sakaguchi, MD, PhD[6]

BACKGROUND: The incidence of cholangiocarcinoma (CCA) is increasing globally. Currently, there is no powerful marker for the diagnosis of CCA, which has led to late diagnosis and poor patient outcome. This study was designed to establish a new monoclonal antibody (MoAb) for detecting a serum marker associated with CCA. **METHODS:** Pooled CCA tissue extracts were immunized to germinal center associated nuclear protein (GANP)-transgenic mice. The antibody-producing hybridomas were prepared and initially screened by using an indirect enzyme-linked immunosorbent assay (ELISA). A positive clone that reacted strongly with CCA serum or tumor tissue extract and failed to react with normal human serum and liver extract was selected. **RESULTS:** An S121 immunoglobulin M MoAb that recognized a novel glycan epitope was obtained. Immunohistochemistry of CCA tissues revealed that the MoAb reacted strongly with hyperplastic/dysplastic and neoplastic bile ducts but not with normal bile ducts. In addition, experiments demonstrated that mucin 5AC (MUC5AC) is a core glycoprotein for the S121 epitope. A sandwich ELISA using soybean agglutinin and an S121 MoAb was developed for detecting S121 reactive antigen in patient sera. The level of serum S121 from patients with CCA was reduced significantly after tumor removal, indicating the tumor origin of this antigen. The test was able to distinguish patients with CCA from healthy individuals, active *Opisthorchis viverrini*-infected individuals and patients with various gastrointestinal cancers, hepatoma, and benign hepatobiliary diseases with 87.63% sensitivity, 89.58% specificity, an 80.95% positive predictive value, and a 93.47% negative predictive value. Moreover, high serum S121 levels were related to a poor patient outcome. **CONCLUSIONS:** The sugar antigen recognized by S121 MoAb is a new serum marker for the diagnosis and prognosis of CCA. **Cancer 2011;000:000–000. © 2011 American Cancer Society.**

KEYWORDS: cholangiocarcinoma, tumor marker, enzyme-linked immunosorbent assay, carbohydrate marker, mucin, mucin 5AC.

Cholangiocarcinoma (CCA) is a rare cancer in Western countries but is considered the major public health problem in the northeast of Thailand, where the incidence of CCA is highest in the world.[1] With unknown factors as the cause, the incidence and mortality rate of CCA are increasing globally.[1-3] CCA is a slow-growing but highly metastatic tumor, which leads to the high mortality rate. Most patients present late and have a median survival of months. The late detection and poor survival after diagnosis has led a need for more powerful markers or techniques for the early diagnosis of CCA. Currently, complete resection is the therapy of choice; however, the difficulty in establishing the diagnosis of CCA preoperatively limits the number of successful treatments. Therefore, the availability of a rapid and formal proof of malignancy by using less invasive procedures, such as a serum marker, remains a constant goal in the diagnosis of CCA.

Corresponding author: Sopit Wongkham, PhD, Department of Biochemistry, Faculty of Medicine, Khon Kaen University, Khon Kaen 40002, Thailand; Fax: (011) 66-43-348-386; sopit@kku.ac.th and Nobuo Sakaguchi, MD, PhD, Department of Immunology, Graduate School of Medical Sciences, Kumamoto University, Kumamoto, 860-8556, Japan; Fax: (011) 81-96-373-5138; nobusaka@kumamoto-u.ac.jp

[1]Department of Biochemistry, Faculty of Medicine, Khon Kaen University, Khon Kaen, Thailand; [2]Liver Fluke and Cholangiocarcinoma Research Center, Faculty of Medicine, Khon Kaen University, Khon Kaen, Thailand; [3]Department of Tumor Genetics and Biology, Graduate School of Medical Sciences, Kumamoto University, Kumamoto, Japan; [4]Department of Pathology, Faculty of Medicine, Khon Kaen University, Khon Kaen, Thailand; [5]Research Center for Medical Glycoscience, National Institute of Advanced Industrial Science and Technology, Ibaraki, Japan; [6]Department of Immunology, Graduate School of Medical Sciences, Kumamoto University, Kumamoto, Japan

We thank Prof. James Will for assistance with the English-language presentation of this article.

N. Sakaguchi is a member of the Global Centers of Excellence Program of Acquired Immunodeficiency Syndrome Research in Japan.

DOI: 10.1002/cncr.25912, **Received:** October 23, 2010; **Revised:** December 7, 2010; **Accepted:** December 7, 2010, **Published online** in Wiley Online Library (wileyonlinelibrary.com)

There are several serum markers for demonstrating CCA, such as carcinoembryonic antigen (CEA),[4,5] carbohydrate antigen 19-9 (CA 19-9), biliary alkaline phosphatase,[6] and serum mucin 5AC (MUC5AC).[7-9] The questions about their overall accuracy, however, limit the use of these markers for early detection. Moreover, patients without cancer may harbor low levels of these markers in blood. The discovery of a new CCA-associated marker with high sensitivity and specificity remains an important objective.

Protein-based markers potentially are powerful, because they are amenable to simple blood tests and can be tested with routine assays. The monoclonal antibody (MoAb) approach has been used for investigating new markers in several cancers.[10,11] This attractive approach not only aids in the discovery of antigens or markers but also provides a tool for generating several marker-detection methods; moreover, it holds out the possibility of identifying a therapeutic bullet.[12] In the current report, we describe a new MoAb, S121, which specifically detects carbohydrate antigens in tumor tissues and sera from patients with CCA. The epitope is observed as a sugar moiety of mucin MUC5AC. A lectin-captured enzyme-linked immunosorbent assay (ELISA) was developed to determine the level of S121-specific carbohydrate markers in serum. We also explored the potential for using this assay as a diagnostic and prognostic marker for CCA.

MATERIALS AND METHODS

Tissues and Serum

Paraffin-embedded liver tissues and sera from patients with CCA were obtained from the Specimen Bank of the Liver Fluke and Cholangiocarcinoma Research Center, Faculty of Medicine, Khon Kaen University, Thailand. Informed consent was obtained from each patient, and the study protocol was approved by the Ethics Committee for Human Research, Khon Kaen University (HE450525 and HE471214). Preoperative sera were obtained from 97 patients with CCA, 43 patients with benign hepatobiliary diseases and 47 patients with gastrointestinal cancers (12 stomach cancers, 9 pancreatic cancers, 13 colon cancers, 3 carcinomas of the ampulla of Vater, and 10 hepatomas). Preoperative and postoperative serum samples (> 3 months postsurgery) were obtained from 17 patients with CCA. Serum samples from 52 patients who had active opisthorchiasis and from 51 healthy individuals were included as controls. All serum samples were stored at −20°C until analysis.

All cancer specimens were obtained from patients with histologically proven disease. Tumor staging was classified according to the American Joint Committee on Cancer classification and staging system.[13] The diagnosis of benign hepatobiliary disease was based on clinical and histologic records. Opisthorchiasis was defined for asymptomatic individuals who had normal serum liver function tests and had positive detection of *Opisthorchis viverrini* eggs in their feces. Serum samples from healthy individuals were obtained from visitors at the hospital who attended an annual health checkup and were age-matched (based on their average age) with the patients with CCA.

Establishment of S121 MoAb

Two germinal center associated nuclear protein (GANP)-transgenic (Ganp^{Tg}) mice[14] were injected intraperitoneally with 50 μg of pooled CCA tumor homogenates (n = 5) in complete Freund adjuvant. Two weeks later, tumor homogenates (50 μg) in incomplete Freund adjuvant were injected subcutaneously. Two weeks after the second boost, the antigen (50 μg) in incomplete Freund adjuvant was prefusion boosted, and cell fusion was performed 4 days later. The antibody-producing hybridomas initially were screened by using a standard, indirect ELISA in pooled sera from patients with CCA or healthy individuals diluted 1:1000 or in crude extracts of CCA tissue or normal liver tissue at a concentration of 50 μg protein/mL as antigen.

A positive clone (S121 MoAb) was selected that reacted strongly with CCA serum or tumor tissue extract but failed to react with normal human serum and normal human liver tissue extract. Large amounts of S121 MoAb were produced in ascetic fluids according to the standard protocol. Briefly, after priming the mice with pristine (Sigma Chemical Company, St. Louis, Mo), the hybridoma was injected intraperitoneally into Balb/c-nude mice (Charles River Japan, Yokohama, Japan) to produce the ascetic fluids. The S121 MoAb was obtained from the ascetic fluids of the mice and further purified using a KAPTIV-M immunoglobulin M (IgM) purification column (Technogen, Piana di Monte Verna, Italy) according to the manufacturer's instructions.

Immunohistochemistry of CCA Tissues Using S121 MoAb

Detection of S121-reactive antigen in CCA tissue sections with the indirect immunoperoxidase method was performed according to the standard protocol. After nonspecific binding was blocked, the sections were incubated

with 5 μg/mL of S121 MoAb at room temperature overnight and with 1:500 horseradish peroxidase (HRP)-conjugated goat antimouse IgM (Southern Biotechnology, Birmingham, Ala) for 1 hour. The immunoreactivity was developed with diaminobenzidine tetrahydrochloride (Sigma Chemical Company) and 0.1% H_2O_2 in 50 mmol/L Tris-HCl, pH 7.8. Sections that were incubated with phosphate-buffered saline (PBS) instead of S121 MoAb were used as negative controls. Anti-MUC1 antibody (Invitrogen, Carlsbad, Calif) was used as a protein-specific antibody control followed by EnVision-system-HRP (Dako, Glostrup, Denmark). The staining frequency of S121-specific antigen was scored semiquantitatively on the basis of the percentage of positive cells as negative (0% positive cells), 1+ (1%-25% positive cells), 2+ (26%-50% positive cells), or 3+ (>50% positive cells).

Characterization of S121-Reactive Epitope

To determine whether the immunoepitope of S121 MoAb was a protein or glycan moiety, protein antigen was digested by trypsin (Invitrogen) or proteinase K (Sigma Chemical Company), whereas the sugar moieties were destroyed by treatment with sodium periodate ($NaIO_4$) (Sigma Chemical Company).[15-17] After deparaffinization and rehydration, the CCA tissue sections were treated either with 10 μg/mL trypsin or 10 μg/mL proteinase K at 37°C, for 1 hour or with 20 mmole/L $NaIO_4$ at 37°C for 2 hours. After washing with PBS, the sections were processed further for immunohistochemistry according to the standard protocol.

For characterization of the antigen epitope in serum, pooled sera (1 mg/mL) from 10 patients with CCA who had different histologic types was serially diluted 2-fold in distilled water, and 1 μL of each diluted sample was dotted onto a nitrocellulose membrane. After drying at room temperature, the membrane was treated with 10 μg/mL trypsin or proteinase K at 37°C for 1 hour. For deglycosylation, the membrane was incubated with 20 mmole/L $NaIO_4$ in 50 mM sodium acetate buffer, pH 4.5, at 37°C for 2 hours. Then, the membrane was washed 3 times for 10 minutes each with 0.3% Tween-20 in PBS (TPBS) and incubated with 5% skim milk in PBS for nonspecific blocking at 37°C for 1 hour. After 3 washings for 10 minutes each in TPBS, the membrane was incubated for 1 hour with 0.5 μg/mL S121 MoAb in TPBS and with 1:10,000 HRP-conjugated goat antimouse IgM at room temperature for 1 hour. Then, the membrane was developed with the Enhanced Chemiluminescence (ECL) Plus Western Blotting Detection System (GE Healthcare, Buckinghamshire, United Kingdom). The images of ECL signals were taken with an ImageQuant 400 image analyzer and were analyzed using ImageQuant TL analysis software (GE Healthcare).

Gel-Filtration Chromatography

To determine the apparent molecular weight of S121 antigen, pooled sera from patients with CCA (100 μL) were fractionated on a 0.5 × 10 cm sepharose-6B gel-filtration chromatography column (Pharmacia Biotech, Uppsala, Sweden) using 25 mM sodium phosphate buffer, pH 7.4, in 150 mM NaCl with a constant flow rate of 0.3 mL per minute. The 0.5-mL eluted fractions were collected, and the absorbance at 280 nm was determined. The level of S121-specific antigen in each fraction was determined with a soybean agglutinin (SBA)-captured ELISA using S121 MoAb.

Sodium Dodecyl Sulfate-Polyacrylamide Gel Electrophoresis and Immunoblot

Pooled sera (30 μg) from patients with CCA were placed on 4% sodium dodecyl sulfate (SDS)-polyacrylamide gels and electrophoresed at 20 mA for 2 hours in SDS-polyacrylamide gel electrophoresis (SDS-PAGE) running buffer according to the method published by Laemmli.[18] Then, the proteins were transferred onto a polyvinylidene fluoride membrane and probed by S121 MoAb as described above (see Characterization of S121-Reactive Epitope).

Glycoconjugate Microarray

The S121-specific sugar was analyzed by using a glycoconjugate microarray that consisted of 98 known sugar compounds as described previously.[19,20] Indocarbocyanine-labeled antimouse IgM (Jackson ImmunoResearch Laboratories, West Grove, Pa) was preincubated with 1 μg/mL S121 MoAb in a probing buffer (25 mM Tris–HCl, pH 7.4; 0.8% NaCl; 1% Triton-X; 1 mM $MnCl_2$; and 1 mM $CaCl_2$) to yield a final dilution of 1:2000. The mixture (100 μL) was applied to the glycoconjugate microarray and incubated at 20°C for 3 hours. The microarray was analyzed by using an evanescent-field fluorescence-assisted scanner (SC-profiler; GP Biosciences, Yokohama, Japan).

Identification of S121 Antigen

Pooled serum samples from patients with CCA were used as a source of S121 antigen. First, albumin and immunoglobulin were depleted from the pooled sera using the

Proteo Extract Albumin/IgG Removal Kit (Calbiochem, Darmstadt, Germany) according to the manufacturer's instructions; then, they were passed through a 0.2-mL S121-immunobilized agarose bead column. The unbound proteins were washed with a ×10 column volume of PBS. The bound protein was eluted with 1 × SDS-PAGE sample buffer and further separated by 4% SDS-PAGE.[18] The pooled serum samples from healthy individuals were processed in the same manner and were used as controls (the S121-negative sample). Gel from the S121-reactive band in patient sera and the corresponding gel from healthy individuals were excised for mass spectroscopy.

Mass Spectrometry

Samples were in-gel digested with trypsin. The digested peptides were desalted by using Zip Tips C18 (Millipore; Bedford, Mass) and were analyzed with nanoelectrospray ionization liquid chromatography (LC)/tandem mass spectrometry (MS/MS) using the LC Packings Ultimate instrument on a QSTAR Pulsar i mass spectrometer (Applied Biosystems/MDS SCIEX, Foster City, Calif). The identified peptide was searched by using the Mascot search engine (Matrix Science, Tokyo, Japan). The proteins that were identified in CCA samples were subtracted from the proteins that were identified in controls.

Lectin-Captured ELISA for S121-Specific Antigens in Sera From Patients With CCA

Fifty microliters of 40 μg/mL SBA (Sigma-Aldrich, Inc., St. Louis, Mo) in 50 mM carbonate buffer, pH 9.6, were coated into an individual well of a 96-well microtiter plate (Corning Incorporated, Corning, NY). After overnight incubation at 4°C in a moisture chamber, the plate was washed 5 times with 0.05% Tween-20 in normal saline. Unbinding sites were blocked with 200 μL of 2% bovine serum albumin (BSA) in 0.05% Tween-20 in PBS (PBST) at 37°C for 1 hour. After washing, serum samples (1:10 dilution; 50 μL) in 1% BSA-PBST were added, incubated at 37°C for 1 hour, then incubated with 50 μL of 1 μg/mL S121 MoAb for 1 additional hour. After washing, 50 μL of 1:4000 HRP-conjugated goat anti-mouse-IgM were added and incubated at 37°C for 1 hour. After washing, freshly prepared 3,3′,5,5′-tetramethyl benzidine (Sigma–Aldrich Inc.) substrate solution (100 μL) was added, and the plate was incubated in the dark for 15 minutes at room temperature; then, 50 μL of 2N sulfuric acid were added to stop the reaction. The optical density was read at 450 nm. All samples were processed in duplicate.

MUC5AC-S121 Sandwich ELISA

To determine whether S121 antigen has a glycan moiety on MUC5AC in serum, a sandwich ELISA using anti-MUC5AC MoAb (clone 22C5)[7] and S121 MoAb was performed. Anti-MUC5AC MoAb (10 μg/mL) was coated onto a 96-well microtiter plate overnight. The subsequent processes were similar to those described for the lectin-captured ELISA.

Statistical Analysis

Statistical analysis was performed using the SPSS software package (version 16.0; SPSS, Chicago, Ill) and SigmaStat software (version 3.1; Systat Software, San Jose, Calif). The S121-specific antigens in sera from patients with CCA were compared with those from the control groups using the Mann-Whitney *U* test. The chi-square test was used to compare the differences in clinicopathologic findings from patients with CCA. A receiver operating characteristic (ROC) curve was constructed to compare the ability of serum S121 antigen to distinguish between the patients with CCA and the control groups.[21] The Youden index was used to select a cutoff value for the optical density (OD) that would indicate the diagnostic values of the test. Patient survival was calculated from the time of surgical resection to death. Survival analyses were performed using the Kaplan-Meier method, and survival was compared using the log-rank test. All P values $< .05$ were considered statistically significant.

RESULTS

More than 400 antibody-producing clones were screened. Of these, a MoAb designated S121 was identified that had high reactivity to pooled sera from patients with CCA but not to sera from healthy individuals. The subclass of this MoAb was named IgM/k.

S121-Specific Antigen Is Highly Expressed in Neoplastic Bile Ducts of CCA Tissue

Immunohistochemistry for S121-specific antigens was performed in 45 histologically proven CCA tumor tissues. Hepatocytes and almost all normal bile duct epithelial cells had negative immunoreactivity for the S121-specific antigen (Fig. 1A), whereas premalignant (Fig. 1B) and malignant (Fig. 1C,D) bile ducts exhibited strong positive staining. Forty-two of 45 CCA tissues (93%) had high reactivity that was both intense and frequent. Almost all

S121-reactive staining was distributed diffusely in the cytoplasm and densely at the apical surface. Some Kupffer cells and inflammatory cells exhibited positive staining. There was no statistical correlation between S121-positive tissues and tumor staging or histologic type among patients with CCA (data not shown).

S121 MoAb Recognizes High-Molecular-Weight Antigen in Sera

To identify the antigen of S121 MoAb, pooled serum samples from patients with CCA were fractionated based on their molecular weight using Sepharose 6B column chromatography. The S121-reactive fractions were observed mainly in the void volume (excluded fraction), suggesting a high molecular weight of S121-reactive antigen, as indicated in Figure 2A. An immunoblot analysis of serum proteins after 4% SDS-PAGE using S121 MoAb revealed an intense band at the top of the gel with an apparent molecular weight > 500 kDa (Fig. 2B).

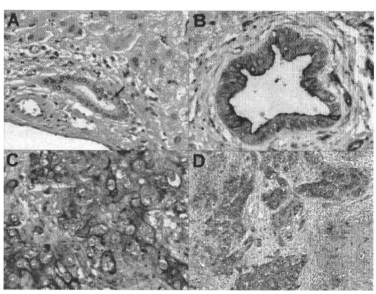

Figure 1. These photomicrographs illustrate the immunoperoxidase staining of S121 monoclonal antibody (mAb) in tissue samples of cholangiocarcinoma (CCA). (A) Normal bile duct epithelium did not stain with the S121 mAb (arrow), whereas S121-positive staining was observed in (B) hyperplasia/dysplasia and (C,D) CCA bile duct epithelium (original magnification, × 400 in A-C, × 100 in D).

S121 MoAb Recognizes Carbohydrate Moieties of the Antigen

Immunoblotting of serum samples from patients with CCA using S121 MoAb revealed positive reactivity in specimens that were treated with trypsin or proteinase K. In contrast, immunoreactivity was diminished in samples that were treated with sodium periodate (Fig. 3A). Similar observations were obtained with the immunohistochemistry of S121 when sections of tissue from CCA tumors were treated with trypsin, proteinase K, or sodium periodate (Fig. 3B). Positive immunohistochemical staining of S121 was retained after the protein antigens were digested with trypsin or proteinase K, whereas the signal was reduced when the sugar moieties were destroyed with sodium periodate. These results indicate the significance of the carbohydrate moieties as immunoepitopes of S121 MoAb. To demonstrate the specificity of trypsin, proteinase K, and sodium periodate treatments, the anti-MUC1 antibody, which recognizes protein fractions, was used instead of S121 MoAb. Immunoreactivity for anti-MUC1 was the reverse of what we observed for S121 MoAb. Positive immunostaining for anti-MUC1 antibody was observed in samples that were treated with sodium

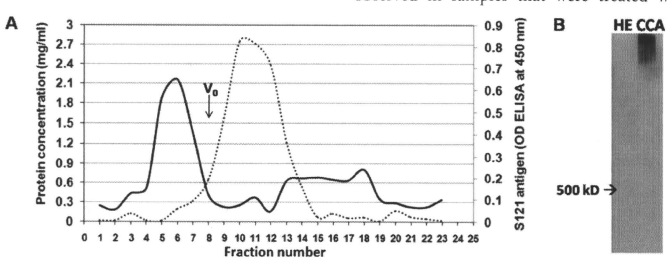

Figure 2. The S121 epitope was identified in high-molecular-weight protein fractions. (A) Pooled serum samples from patients with cholangiocarcinoma (CCA) were fractionated on a Sepharose 6B column, and the absorbance of protein at 280 nm (dotted line) and S121-specific antigen levels (solid line) were determined. S121 antigen was observed mainly in the void fractions. (B) This immunoblot of pooled sera from healthy individuals (HE) was compared with serum samples from patients with CCA. The S121 antigen was identified only in sera from patients with CCA at an apparent molecular weight >500 kDa. OD indicates outer diameter; ELISA, enzyme-linked immunosorbent assay.

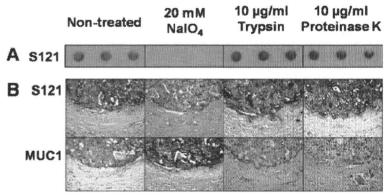

Figure 3. These images characterize S121-reactive antigen in (A) pooled serum samples from patients with cholangiocarcinoma and (B) tumor tissues that were treated either with protease (trypsin and proteinase K) or with periodate oxidization as described in the text (see Materials and Methods). After treatment, S121 antigen levels in each sample were determined using (A) immunoblotting and (B) immunohistochemistry. A monoclonal antibody against the protein part of mucin 1 (MUC1) was used as a control for the specific reactions of enzyme and sodium periodate treatment.

periodate, but immunostaining was reduced markedly in samples that were treated with trypsin or proteinase K (Fig. 3B). Taken together, these findings strongly suggest that the S121 MoAb recognizes an epitope of carbohydrate itself or an epitope that is associated with carbohydrate.

The potential structure of the glycan unit recognized by S121 MoAb was investigated further using a glycoconjugate microarray.[19,20] Of 100 glycan structures that were immobilized in the array, no known glycan moiety or common tumor markers reported as CCA marker, such as sialyl-Lewis A (sLe^a), Le^y, Le^x, sLe^x, sialyl-Tn antigen, etc, reacted with S121 MoAb. Therefore, it is probable that S121 MoAb recognizes a new carbohydrate-associated antigen that has not yet been identified.

MUC5AC Mucin Was Identified as the Core Glycoprotein of Carbohydrate Moieties Recognized by S121 MoAb

To identify the core protein of the S121 sugar epitope, S121 antigen in sera from patients with CCA was purified by S121 MoAb-affinity chromatography and separated further by SDS-PAGE. The LC/MS/MS analysis revealed that 14 peptide were sequences generated from tryptic digested CCA serum coinciding with those of MUC5AC (Fig. 4A). To confirm that the S121-recognizing glycan epitope was a component of MUC5AC mucin, a sandwich ELISA using anti-MUC5AC (22C5-MoAb) and S121 MoAb was performed. The reactivity of S121 MoAb obtained from the sandwich ELISA system using MUC5AC antibody (22C5 MoAb) and S121 MoAb was similar to that of obtained with the lectin-captured ELISA with S121 MoAb, as illustrated in Figure 4B. In addition, $NaIO_4$-treated serum samples exhibited lower reactivity for S121 MoAb obtained from the anti-MUC5AC captured sandwich ELISA system. This result indicated that the sugar moieties of MUC5AC mucin are the epitopes recognized by S121 MoAb.

Value of Serum S121 Antigen as a Diagnostic Indicator of CCA

A lectin-capture ELISA was developed to determine the levels S121-specific antigen in serum. Checkerboard studies were performed to determine the optimal concentrations of S121 MoAb and to test sera with a fixed dilution (1:4000) of HRP-conjugated goat antimouse-IgM. Plates were coated with various concentrations of SBA (10-50 μg/mL) and reacted with different dilutions of test sera. The ELISA system using 50 μL of 40 μg/mL SBA at 1:10 dilution of sera and using 50 μL of 1 μg/mL S121 MoAb yielded the highest absorbance for CCA sera and the lowest absorbance for normal, healthy sera. Therefore, this system was used for subsequent studies.

The levels of S121 antigen determined by SBA-captured ELISA in serum samples from patients with CCA and from the control groups are illustrated in Figure 5A. The median serum S121 value was elevated significantly in samples from patients with CCA compared with the median value in samples from the control groups (patients with gastrointestinal cancer, patients with benign hepatobiliary diseases, patients with opisthorchiasis, and healthy individuals; $P < .001$). An analysis of the ROC curve was performed to determine the best cutoff S121 antigen value that distinguished patients with CCA from individuals in the control groups. On the basis of ROC curve analysis, an area under the curve of 0.956 (95% confidence interval [CI], 0.934-0.977) is illustrated in Figure 5B. Using a cutoff OD of 450 nm at an area under the curve of 0.11 produced sensitivity of 87.63% (85 of 97 patients) and specificity of 89.58% (172 of 192 patients) with a positive predictive value of 80.95% (85 of 105 patients) and a negative predictive value of 93.47% (172 of 192 patients). Serum S121 levels were not associated with age, sex, histopathology, or tumor staging among the patients as determined by univariate analysis (data not shown).

To demonstrate the tumor origin of the S121 antigen identified in serum, the association of S121 antigen detected in serum and tumor tissues was investigated further. Serum levels of S121 antigen from patients with CCA were determined before and after they underwent tumor resection. Seventeen patients with CCA who did

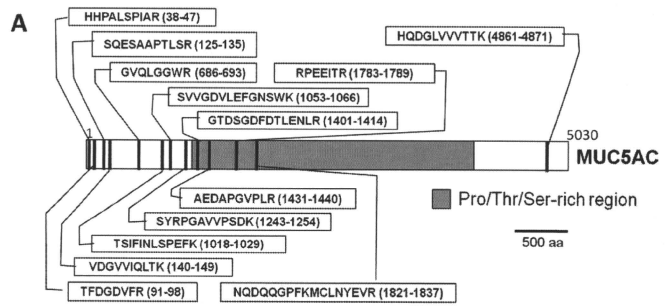

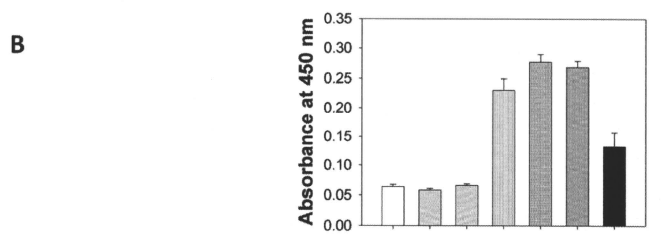

Detectors	HRP conjugated anti-IgM	-	+	+	-	+	+	+
	HRP conjugated SBA	+	-	-	+	-	-	-
Primary Ab	S121 MoAb	-	-	-	-	+	+	+
Antigens	CCA pooled serum	-	-	-	+	+	+	-
	$NaIO_4$ treated CCA pooled serum	-	-	-	-	-	-	+
Captures	SBA	-	+	-	-	+	-	-
	Anti-MUC5AC (22C5)	+	-	+	+	-	+	+

Figure 4. (A) The identified peptides from S121-purified antigen mapped on mucin 5AC (MUC5AC) are shown. Most peptides were hit at the N-terminus of MUC5AC, which is not a highly glycosylated part. Pro indicates proline; Thr, threonine; Ser, serine. (B) The presence of MUC5AC was determined in sera from patients with cholangiocarcinoma (CCA) using a sandwich enzyme-linked immunosorbent assay (ELISA) (lane 4, anti-MUC5AC and horseradish peroxidase [HRP]-conjugated soybean agglutinin [SBA]) and yielded results similar to those obtained with a lectin-captured ELISA of S121 antigen (lane 5, SBA and S121 MoAb) and from MUC5AC captured with an S121 MoAb ELISA (lane 6, anti-MUC5AC and S121 MoAb). Lanes 1, 2, and 3 were negative controls for each ELISA system. Treatment of serum with $NaIO_4$ at 37°C for 2 hours (lane 7) reduced the reactivity of S121 MoAb obtained from the anti-MUC5AC-captured sandwich ELISA system. IgM indicates immunoglobulin M; Ab, antibody.

not receive any treatment after tumor resection were included in this study. The elevated S121 level observed as OD in preoperative serum samples from patients with CCA was 0.324 ± 0.134 and decreased significantly to 0.239 ± 0.065 after tumor removal ($P < .001$) (Fig. 5C).

High Serum S121 Antigen Indicates a Worse Prognosis for Patients With CCA

In total, 97 patients with CCA who had different demographic characteristics were included in this study (Table 1). Patients with CCA were categorized according to their

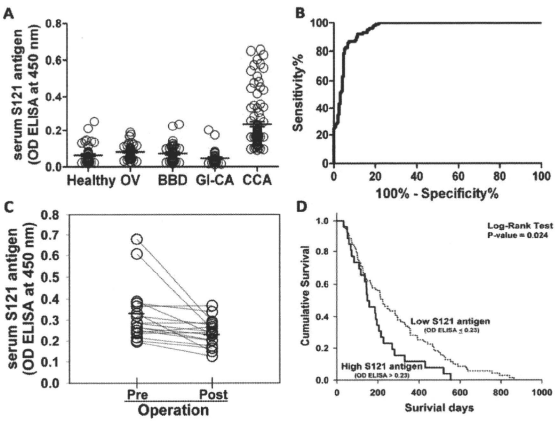

Figure 5. The determination of S121 antigen levels in serum is illustrated. (A) S121 antigen levels in sera from patients with cholangiocarcinoma (CCA) (n = 97) were determined by using a soybean agglutinin-captured enzyme-linked immunosorbent assay (ELISA) and were compared with the levels in healthy individuals (HE) (n = 51), in liver fluke-infected patients (OV) (n = 52), in patients with benign biliary diseases (BBD) (n = 43), and in patients with other gastrointestinal cancers (GI-CA) (n = 47). OD indicates outer diameter. (B) Receiver operating characteristic (ROC) analysis yielded an area under the ROC curve of 0.956 (95% confidence interval, 0.934-0.977) and a *P* value < .001. (C) The level of S121 antigen decreased significantly after tumor removal (n = 17; *P* < .001; Wilcoxon signed-rank test). (D) Kaplan-Meier analysis indicated that patients with CCA who had low serum S121 antigen levels (OD of ELISA, ≤0.23) had better survival than patients who had high serum S121 levels (OD of ELISA, >0.23; *P* = .024; log-rank test).

Table 1. Demographic Characteristics of Patients With Cholangiocarcinoma

Characteristic	No. of Patients (%)
Age, y	
≤56	45 (46.4)
>56	52 (53.6)
Sex	
Men	69 (71.1)
Women	28 (28.9)
Histopathology	
Papillary	22 (22.7)
Nonpapillary	75 (77.3)
Tumor stage	
I-III	14 (14.4)
IVA-IVB	83 (85.6)

mean serum S121 levels of the CCA into a group with low serum S121 (OD, ≤0.23 nm) and a group with high serum S121 (OD, >0.23 nm). If patients survived for <30 days, then their deaths were considered perioperative, and those patients were excluded from the analysis. A log-rank analysis indicated that patients with CCA who had low serum S121 antigen levels had significantly better survival than the patients who had high serum S121 antigen levels (*P* = .024) (Fig. 5D). The respective median survival was 224 ± 21 days (95% CI, 183-265 days) and 148 ± 52 days (95% CI, 95-200 days) for CCA patients in the low and high serum S121 groups, respectively.

DISCUSSION

In this report, we detail the discovery of a new MoAb that specifically reacts with a novel carbohydrate moiety of a high-molecular-weight glycoprotein(s) that was identified in tumor tissues and sera from patients with CCA. By using crude extracts from pooled CCA tissues as immunogens for generating MoAbs and using serum samples from patients with CCA as antigens for MoAb screening, the S121 MoAb, which recognizes a novel carbohydrate epitope on a tumor-originated antigen, was established. We demonstrated that the recognized S121 antigen is the carbohydrate moiety of a high-molecular-weight glycoprotein(s). Antigenicity of the S121antigen was abolished when the antigen was